[1]

MODELING AND SIMULATION WITH OPERATOR SCALING: EXTENDED VERSION WITH ADDITIONAL EXAMPLES

SERGE COHEN, MARK M. MEERSCHAERT, AND JAN ROSIŃSKI

Abstract. Self-similar processes are useful models for natural systems that exhibit scaling. Operator scaling allows a different scale factor in each coordinate. This paper develops practical methods for modeling and simulation. A simulation method is developed for operator scaling Lévy processes, based on a series representation, along with a Gaussian approximation of the small jumps. Several examples are given to illustrate the range of practical applications. A complete characterization of symmetries is given in two dimensions, for any exponent and spectral measure, to inform the choice of these model parameters. The paper concludes with some extensions to general operator self-similar processes.

1. Introduction

Self-similar processes form an important and useful class, favored in practical applications for their nice scaling properties, see for example the recent books of Embrechts and Maejima [10] and Sheluhin et al. [50]. The subject was popularized by Mandelbrot [26]; see [1] for additional applications to electrical engineering, image processing, computer network traffic, finance, and astrophysics. Recall that a stochastic process $\mathbf{X} = \{X(t)\}_{t\ge 0}$ taking values in $\mathbb{R}^d$ is *self-similar* if

$$\{X(ct)\}_{t\ge 0} \stackrel{fd}{=} \{c^\beta X(t)\}_{t\ge 0} \tag{1.1}$$

at every scale $c > 0$. Here $\stackrel{fd}{=}$ indicates equality of finite dimensional distributions, and we assume $\mathbf{X}$ is stochastically continuous with $X(0) = 0$. The parameter $\beta > 0$ is often called the Hurst index [15]. Operator self-similar processes allow the scaling factor (Hurst index) to vary with the coordinate. Therefore, a process $\mathbf{X}$ as above is said to be *operator self-similar (o.s.s.)* if there exists a linear operator $B \in \mathrm{GL}(\mathbb{R}^d)$ (i.e., an invertible $d \times d$ matrix) such that

$$\{X(ct)\}_{t\ge 0} \stackrel{fd}{=} \left\{c^B X(t)\right\}_{t\ge 0}, \tag{1.2}$$

for all $c > 0$, where the matrix power $c^B := \exp(B \log c)$. The linear operator B in (1.2) is called an *exponent* of the operator self-similar process $\mathbf{X}$. If $B = \beta I$ for some $\beta > 0$, then $\mathbf{X}$ is self-similar. If B is diagonal, then the marginals of $\mathbf{X}$ are self-similar, and the Hurst index can vary with the coordinate. This is important in modeling many real world phenomena.

[1] *AMS classification (2000)*: 60G51, 60G52, 68U20, 60F05.

Date: May 17, 2011.

Key words and phrases. Lévy processes, Gaussian approximation, shot noise series expansions, simulation, tempered stable processes, operator stable processes.

M. M. Meerschaert was partially supported by NSF grants DMS-0803360 and EAR-0823965. J. Rosiński was partially supported by NSA grant MSPF-50G-049. S. Cohen wishes to thank the Department of Mathematics, University of Tennessee, for their hospitality during a visit that initiated this project.

Park and Cushman [38] use an operator self-similar model for anomalous dispersion in porous media, and develop the associated Fokker-Planck equations for the motion of individual particles. Because the porous medium is not isotropic, the scaling properties vary with direction, see also [31, 51]. Molz et al. [37] discuss connections to the multiscaling structure of natural aquifers. Rachev and Mittnik [41] show that the scaling index will vary between elements of a portfolio containing different stocks. Similar results were obtained in [33] for exchange rates. Jansen and de Vries [13] use these models to explain the 1987 stock market crash, see also Loretan and Phillips [21]. In tick-by-tick analysis of financial data, it is useful to consider the waiting time between trades and the resulting price change as a two dimensional random vector. Scalas et al. [35, 49] show that different indices apply to price jumps and waiting times. Park and Cushman [38] employ an operator self-similar model for the chaotic dynamics of self-motile colloid particles at the microscale, where the sample paths trace the movements of individual microbes. Results and further references on o.s.s. processes can be found in [10, Chapter 9] and [30, Chapter 11], see also the pioneering work of Hudson and Mason [14].

The main goal of this paper is to provide practitioners with the necessary tools for building models with operator scaling. We focus on operator self-similar Lévy processes, a type of operator stable process. Section 2 describes this class, with an emphasis on parameterization. An operator self-similar Lévy process has two parameters: a matrix exponent; and a spectral measure. Roughly speaking, the exponent determines the scaling, and the spectral measure codes dependence between the different coordinates. Section 3 presents a method for simulating sample paths, based on a shot noise representation. A Gaussian approximation of the small jumps accelerates convergence of the method. Theorem 3.1 justifies this method, and provides error bounds. The simulation algorithm facilitates numerical experiments to validate the model, once parameters are chosen. Section 4 presents a number of examples to illustrate the broad range of applications. These examples also highlight the effect of the exponent and spectral measure on sample path behavior, to provide a basis for choosing those parameters in practical applications. Section 5 shows how the exponent and spectral measure interact to determine the symmetries. Symmetry is an important modeling consideration, and a useful guide to model selection. Theorem 5.1 provides a complete classification of the possible symmetry groups in two dimensions, in terms of the exponent. Theorem 5.2 shows how the exponent interacts with the spectral measure to determine the symmetries, and then Remark 5.3 shows how to explicitly construct an operator self-similar Lévy process with any given exponent and any admissible symmetry group, by selecting the appropriate spectral measure. Finally, Section 6 provides some extensions to general operator self-similar processes.

2. Operator stable processes

This section recalls some basic facts about operator stable Lévy processes, with an emphasis on parameterization. An operator stable Lévy process evolves in a d-dimensional vector space. It has two parameters: a linear operator defined by a $d \times d$ matrix, called an exponent; and a finite measure on the $d-1$ dimensional unit sphere, called a spectral measure. Roughly speaking, the exponent determines the scaling, and the spectral measure codes dependence between the d different coordinate processes.

We say that a Lévy process $\mathbf{X} = \{X(t)\}_{t\geq 0}$ taking values in $\mathbb{R}^d$ is operator stable with *exponent* $B \in \mathrm{GL}(\mathbb{R}^d)$ if for every $t > 0$ there exists a vector $b(t) \in \mathbb{R}^d$ such that

$$X(t) \stackrel{d}{=} t^B X(1) + b(t) \tag{2.1}$$

where $\stackrel{d}{=}$ means equal in distribution. We say that $\mathbf{X}$ is strictly operator stable when $b(t) = 0$ for all $t > 0$. A Lévy process is operator self-similar if and only if it is strictly operator stable, in which case the exponents coincide [14, Theorem 7]. In general, if $\mathbf{X}$ is operator stable and 1 is not an eigenvalue of the exponent B, then there exists a vector a such that $\{X(t) - at\}_{t\geq 0}$ is strictly operator stable; a complete description of strictly operator stable processes is given by Sato [47]. Henceforth we will always assume that the infinitely divisible distribution $\mu = \mathcal{L}(X(1))$ is full dimensional, i.e., not supported on a lower dimensional hyperplane. The distributional properties of μ determine those of $\mathbf{X}$. Indeed, two Lévy processes $\mathbf{X}$ and $\mathbf{Y}$ have the same finite dimensional distributions if and only if $X(1)$ and $Y(1)$ are identically distributed.

A comprehensive introduction to operator stable laws can be found in the monographs [17] and [30]. The necessary and sufficient condition for a $d\times d$ matrix B to be an exponent of a full operator stable law is that all the roots of the minimal polynomial of B have real parts greater than or equal to $1/2$, and all the roots with real part equal to $1/2$ are simple, see [17, Theorem 4.6.12]. In this work we will assume that the operator stable law μ has no Gaussian component, so that all the roots of the minimal polynomial of B have real parts greater than $1/2$. Since the operator stable law μ is infinitely divisible, with no Gaussian component, its characteristic function can be expressed in terms of the Lévy representation

$$\log \mathbb{E}e^{i\langle y, X(1)\rangle} = i\langle y, x_0\rangle + \int_{\mathbb{R}^d} (e^{i\langle y,x\rangle} - 1 - i\langle y, x\rangle \mathbf{1}_{\{\|x\|\leq 1\}})\, \nu(dx). \tag{2.2}$$

See, e.g., [30, Theorem 3.1.11]. Since μ is full, the smallest linear space supporting the Lévy measure ν is $\mathbb{R}^d$ [30, Proposition 3.1.20].

Next we define the spectral measure. For a given exponent B, consider a norm $\|\cdot\|_B$ on $\mathbb{R}^d$ satisfying the following conditions

(i) for each $x \in \mathbb{R}^d$, $x \neq 0$, the map $t \mapsto \|t^B x\|_B$ is strictly increasing in $t > 0$,
(ii) the map $(t, x) \mapsto t^B x$ from $(0, \infty) \times S_B$ onto $\mathbb{R}^d \setminus \{0\}$ is a homeomorphism,

where $S_B = \left\{x \in \mathbb{R}^d : \|x\|_B = 1\right\}$ is the unit sphere with respect to $\|\cdot\|_B$. There are many ways of constructing such norms. For example, Jurek and Mason [17, Proposition 4.3.4] propose

$$\|x\|_B = \left(\int_0^1 \|s^B x\|^p s^{-1}\, ds\right)^{1/p} \tag{2.3}$$

where $1 \leq p < \infty$ and $\|\cdot\|$ is *any* norm on $\mathbb{R}^d$. If the matrix B is in Jordan form, then Meerschaert and Scheffler [30, Remark 6.1.6] observe that the function $t \mapsto \|t^B x\|$ is regularly varying for any $x \neq 0$. Then it can be shown that $t \mapsto \|t^B x\|_B$ is both strictly increasing, and regularly varying. If B is in Jordan form, with no nilpotent part, then the Euclidean norm satisfies conditions (i) and (ii). Also, if B is in Jordan form on $\mathbb{R}^2$, then it is easy to check that the Euclidean norm satisfies conditions (i) and (ii). Under

conditions (i)-(ii) we have the *polar decomposition*

$$\nu(E) = \int_{S_B} \int_0^\infty \mathbf{1}_E(s^B u) s^{-2}\, ds\lambda(du), \tag{2.4}$$

where λ is a finite Borel measure on S_B called the *spectral measure* of μ. The spectral measure is given by

$$\lambda(F) = \nu(\{x : x = t^B u, \text{ for some } (t,u) \in [1,\infty) \times F\}) \tag{2.5}$$

and then it follows from (2.4) and (2.5) that the spectral measure λ is uniquely determined for a given Lévy measure ν, exponent B, and norm $\|x\|_B$. The choice of $\|\cdot\|_B$ is a matter of convenience. For example, if B is in Jordan form, then the Euclidean norm $\|\cdot\|$ is a natural choice for $\|\cdot\|_B$. Once the coordinate system and norm are fixed, the exponent B and the spectral measure λ determine the operator stable Lévy process, up to a drift term determined by the vector x_0 in (2.2).

3. Accelerated series representation

This section develops an efficient simulation algorithm for operator stable Lévy processes. The main technical advantage of the method is that the large jumps are exactly reproduced, at exactly the correct time points. Let $\mathbf{X} = \{X(t)\}_{t\ge 0}$ be a proper operator stable Lévy process with exponent B, spectral measure λ, no Gaussian component, and characteristic function defined by (2.2) and (2.4). Our simulation algorithm is based on a series representation [44]: For any fixed $T > 0$,

$$X(t) = \sum_{j=1}^{\infty} \left\{ \mathbf{1}_{(0,\,t]}(\tau_j) \left(\frac{\Gamma_j}{T\lambda(S_B)} \right)^{-B} v_j - \frac{t}{T} c_j \right\}, \quad t \in [0,T], \tag{3.1}$$

where $\{\tau_j\}$ is an iid sequence of uniform on $[0,T]$ random variables, $\{\Gamma_j\}$ forms a Poisson point process on $(0,\infty)$ with the Lebesgue intensity measure, $\{v_j\}$ is an iid sequence on S_B with the common distribution $\lambda/\lambda(S_B)$, and

$$c_j = \int_{j-1}^{j} \int_{\|x\|\le 1} x\sigma_r(dx)\, dr, \tag{3.2}$$

with

$$\sigma_r(A) = P\left(\left(\frac{r}{T\lambda(S_B)} \right)^{-B} v_1 \in A \right) \tag{3.3}$$

(see [45, Eq. (5.6)]). The random sequences $\{\tau_j\}$, $\{\Gamma_j\}$, and $\{v_j\}$ are independent. The series (3.1) converges pathwise uniformly on $[0,T]$ with probability one, see [45, Theorem 5.1]. This series expansion falls into a general category of shot noise representations and is a consequence of the polar decomposition (2.4), see remark following [44, Corollary 4.4].

In order to accelerate convergence, the small jumps in (3.1) can be approximated by a Brownian motion [8]. The Gaussian approximation of small jumps allows a fast and accurate simulation of sample paths. Fix $\epsilon \in (0,1]$ and define $\mathbf{N}^\epsilon = \{N^\epsilon(t)\}_{t\in[0,T]}$ by

$$N^\epsilon(t) = \sum_{\Gamma_j \le T\lambda(S_B)/\epsilon} I_{(0,\,t]}(\tau_j) \left(\frac{\Gamma_j}{T\lambda(S_B)} \right)^{-B} v_j. \tag{3.4}$$

It is elementary to check that $\mathbf{N}^\epsilon$ is a compound Poisson process with characteristic function

$$\mathbb{E}\exp i\langle y, N^\epsilon(t)\rangle = \exp\left\{ t\int_{S_B}\int_\epsilon^\infty (e^{i\langle y, s^B u\rangle} - 1)s^{-2}\, ds\lambda(du)\right\}.$$

To see this: Observe that the number of terms M_ϵ in the sum (3.4) is Poisson with mean $\theta_\epsilon = T\lambda(S_B)/\epsilon$; condition on $M_\epsilon = n$ in the characteristic function, noting that $(\Gamma_1/\theta_\epsilon, \ldots, \Gamma_n/\theta_\epsilon)$ is equal in distribution to the vector of order statistics from n IID standard uniform random variables; permute the order statistics; and rewrite the characteristic function as an integral. Thus $\mathbf{N}^\epsilon$ has the Lévy measure

$$\nu^\epsilon(A) = \int_{S_B}\int_\epsilon^\infty \mathbf{1}_A(s^B u)s^{-2}\, ds\lambda(du).$$

The remainder

$$R_\epsilon(t) = X(t) - N^\epsilon(t), \tag{3.5}$$

is a Lévy process independent of $\mathbf{N}^\epsilon$ and $R_\epsilon(1)$ has Lévy measure ν_ϵ of bounded support given by

$$\nu_\epsilon(A) = \int_{S_B}\int_0^\epsilon \mathbf{1}_A(s^B u)s^{-2}\, ds\lambda(du). \tag{3.6}$$

Therefore, all moments of $R_\epsilon(1)$ are finite. A straightforward computation shows that

$$a_\epsilon := \mathbb{E}R_\epsilon(1) = \int_{\|x\|>1} x\,\nu_\epsilon(dx) - \int_{\|x\|\le 1} x\,\nu^\epsilon(dx). \tag{3.7}$$

Then we have

$$X(t) = ta_\epsilon + N^\epsilon(t) + \{R_\epsilon(t) - \mathbb{E}[R_\epsilon(t)]\}.$$

Theorem 3.1 will show that, under certain matrix scaling, the last term $R_\epsilon(t) - \mathbb{E}[R_\epsilon(t)]$ converges to a standard Brownian motion in $\mathbb{R}^d$. Thus, any operator stable Lévy process can be faithfully approximated by the sum of two independent component processes, a compound Poisson and a Brownian motion with drift. The matrix scaling depends on the covariance matrix Σ_ϵ of $R_\epsilon(1)$: A simple computation (see [8, Eq. (2.3)]) yields

$$\begin{aligned}\Sigma_\epsilon &= \mathbb{E}\left[(R_\epsilon(1) - \mathbb{E}[R_\epsilon(1)])(R_\epsilon(1) - \mathbb{E}[R_\epsilon(1)])^\top\right] \\ &= \int_{S_B}\int_0^\epsilon (s^B u)(s^B u)^\top s^{-2}\, ds\lambda(du) = \int_0^\epsilon s^B \Lambda (s^B)^\top s^{-2} ds,\end{aligned} \tag{3.8}$$

where Λ is given by

$$\Lambda = \int_{S_B} uu^\top \lambda(du). \tag{3.9}$$

Recall from Section 2 that, since $\mathbf{X}$ has no Gaussian component,

$$b_* := \min\{b_1, \ldots, b_d\} > \frac{1}{2}, \tag{3.10}$$

where $b_1, \ldots, b_d$ are the real parts of the eigenvalues of B.

Theorem 3.1. *Let* $\mathbf{X}$ *be an operator stable Lévy process with exponent* B *and spectral measure* λ *such that*

$$lin_B(supp\ \lambda) = \mathbb{R}^d, \tag{3.11}$$

where $lin_B(supp\lambda)$ *denotes the smallest* B*-invariant subspace of* $\mathbb{R}^d$ *containing the support of* λ*. Fix* $T > 0$ *and let* $\mathbf{N}^\epsilon$ *be as in* (3.4)*,* $\mathbf{W}$ *be a standard Brownian motion in* $\mathbb{R}^d$ *independent of* $\mathbf{N}^\epsilon$*, and* $\mathbf{a}_\epsilon = \{a_\epsilon t\}_{t\geq 0}$ *be a drift determined by* (3.7)*. Define*

$$A_\epsilon = \epsilon^{-1/2}\epsilon^B\Sigma_1^{1/2} \tag{3.12}$$

where Σ_1 *is given by* (3.8) *with* $\epsilon = 1$*.*

Then, for every $\epsilon \in (0,1]$ *there exists a cádlág process* $\mathbf{Y}_\epsilon$ *such that on* $[0,T]$

$$\mathbf{X} \stackrel{fd}{=} \mathbf{a}_\epsilon + A_\epsilon\mathbf{W} + \mathbf{N}^\epsilon + \mathbf{Y}_\epsilon \tag{3.13}$$

in the sense of equality of finite dimensional distributions and such that for every $\delta > 0$

$$\epsilon^{1/2-b_*+\delta} \sup_{t\in[0,T]} \|Y_\epsilon(t)\| \xrightarrow{\mathbb{P}} 0 \quad as\ \epsilon \to 0 \tag{3.14}$$

where b_* *is given by* (3.10)*.*

Proof. The proof is an application of Theorem 3.1 in [8] (see also Freedman [11]). That theorem requires Σ_ϵ to be nonsingular for all $\epsilon > 0$. In view of the scaling

$$\Sigma_\epsilon = \epsilon^{-1}\int_0^1 (\epsilon\, r)^B\Lambda((\epsilon\, r)^B)^\top\, r^{-2}dr = \epsilon^{-1}\epsilon^B\Sigma_1(\epsilon^B)^\top \tag{3.15}$$

it suffices to show that Σ_1 is nonsingular when (3.11) holds. Let ν_1 be the Lévy measure (3.6) with $\epsilon = 1$ and let

$$L = \mathrm{lin}(\mathrm{supp}\,\nu_1)$$

be the closed linear space spanned by $\mathrm{supp}\,\nu_1$. By [8, Lemma 2.1] it suffices to show that $L = \mathbb{R}^d$. Following [17, Corollary 4.3.5] we have

$$\mathrm{supp}\,\nu_1 = \{x : x = s^B u,\ 0 \leq s \leq 1,\ u \in \mathrm{supp}\,\lambda\}.$$

We will show that L is B–invariant. To this end it is enough to show that if $x = s^B u \in \mathrm{supp}\,\nu_1$, for some $0 < s \leq 1$ and $u \in \mathrm{supp}\,\lambda$, then $Bs^B u \in L$. For any $\theta \in (0,1)$, $(\theta s)^B u \in \mathrm{supp}\,\nu_1$ so that

$$Bs^B u = \lim_{\theta\nearrow 1} \frac{(\theta s)^B u - s^B u}{\log\theta} \in L.$$

Since L is closed and B–invariant and contains the support of λ, $L = \mathbb{R}^d$ by (3.11). Thus Σ_1 is nonsingular.

Theorem 2.2 in [8] shows that the asymptotic normality of $R_\epsilon(t) - \mathbb{E}[R_\epsilon(t)]$ holds if and only if for every $\kappa > 0$ we have

$$\lim_{\epsilon\to 0}\int_{\langle\Sigma_\epsilon^{-1}x,x\rangle>\kappa} \langle\Sigma_\epsilon^{-1}x, x\rangle\, \nu_\epsilon(dx) = 0. \tag{3.16}$$

Using (3.15) we have

$$\begin{aligned}\langle \Sigma_\epsilon^{-1} s^B u, s^B u\rangle &= \epsilon \langle (\epsilon^{-B})^\top \Sigma_1^{-1} \epsilon^{-B} s^B u, s^B u\rangle \\ &= \epsilon \langle \Sigma_1^{-1} \epsilon^{-B} s^B u, \epsilon^{-B} s^B u\rangle \\ &= \epsilon \langle \Sigma_1^{-1} (s/\epsilon)^B u, (s/\epsilon)^B u\rangle\end{aligned}$$

Note that in general $\langle Ax, x\rangle \le \|A\|\|x\|^2 \le C\|A\|\|x\|_B^2$ (for some constant $C > 0$, since all norms on $\mathbb{R}^d$ are equivalent). Then, since $t \mapsto \|t^B u\|_B$ is strictly increasing and $t^B x = x$ when $t = 1$, the above bound shows that

$$\langle \Sigma_\epsilon^{-1} s^B u, s^B u\rangle \le C\epsilon \|\Sigma_1^{-1}\| \|(s/\epsilon)^B u\|_B^2 \ \le C\epsilon \|\Sigma_1^{-1}\|, \tag{3.17}$$

whenever $0 < s \le \epsilon \le 1$ and $u \in S_B$. Since Σ_1 is invertible we know that $c_1 = C\|\Sigma_1^{-1}\| \in (0, \infty)$. Then, for every $\kappa > 0$ and $\epsilon \in (0, 1)$ we have

$$\begin{aligned}&\int_{\langle \Sigma_\epsilon^{-1} x, x\rangle > \kappa} \langle \Sigma_\epsilon^{-1} x, x\rangle \, \nu_\epsilon(dx) \\ &\qquad = \iint_{\{(s,u)\in(0,\epsilon]\times S_B:\ \langle \Sigma_\epsilon^{-1} s^B u, s^B u\rangle > \kappa\}} \langle \Sigma_\epsilon^{-1} s^B u, s^B u\rangle \, s^{-2} \, ds\lambda(du) \\ &\qquad = 0\end{aligned}$$

when $\epsilon < c_1^{-1}\kappa$. Indeed, in view of (3.17) the region of integration is empty for $c_1\epsilon < \kappa$. Therefore, (3.16) trivially holds.

Applying [8, Theorem 3.1] we get (3.13) and that

$$\sup_{t\in[0,T]} \|A_\epsilon^{-1} Y_\epsilon(t)\| \xrightarrow{\mathbb{P}} 0 \quad \text{as } \epsilon \to 0. \tag{3.18}$$

It remains to show (3.14). If $\|\Sigma_1\| = c_2$ then $\|\Sigma_1^{1/2}\| = \sqrt{c_2}$. Since every eigenvalue of $-B$ has real part less than or equal to $-b_*$, [30, Proposition 2.2.11 (d)] implies that for any $\delta > 0$, for some $c_3 > 0$, we have $\|t^{-B} x\| \le c_3 t^{-b_* + \delta} \|x\|$ for all $t \ge 1$ and all $x \in \mathbb{R}^d$. Then $\|s^B\| \le c_3 s^{b_* - \delta}$ for all $s \le 1$. Then for all $0 < \epsilon \le 1$ we have

$$\|A_\epsilon\| \le \epsilon^{-1/2} \|\epsilon^B\| \, \|\Sigma_1^{1/2}\| \le c\epsilon^{-1/2 - \delta + b_*}.$$

where $c = c_3\sqrt{c_2}$. Therefore,

$$\|Y_\epsilon(t)\| \le \|A_\epsilon\| \|A_\epsilon^{-1} Y_\epsilon(t)\| \le c\epsilon^{-1/2 - \delta + b_*} \|A_\epsilon^{-1} Y_\epsilon(t)\|,$$

which together with (3.18) yields (3.14). The proof is complete. □

4. Simulation

This section implements the simulation method of Section 3 for sample paths of an operator stable Lévy process $\{X(t)\}_{t\in[0,T]}$ specified by (2.2) and (2.4). Several examples illustrate the range of behavior possible for an operator scaling model, and illuminate the effect of the exponent B and the spectral measure λ on the sample paths. Theorem 3.1 decomposes $\mathbf{X}$ into the drift $a_\epsilon t$, the large jumps $N^\epsilon(t)$, and a Gaussian approximation of the small jumps. This justifies the approximation

$$X(t) \approx Z_\epsilon(t) := a_\epsilon t + A_\epsilon W(t) + N^\epsilon(t), \tag{4.1}$$

with A_ϵ given by (3.12) and $W(t)$ a standard Brownian motion, to simulate sample paths. The process $\{Z_\epsilon(t)\}_{t\in[0,T]}$ reproduces the large jumps exactly, which is its main technical advantage. The error in the Gaussian approximation of small jumps is given by the remainder term $\mathbf{Y}_\epsilon$ in (3.13), whose supremum converges to zero in probability at a polynomial rate described by (3.14) as the number of large jumps increases or, equivalently, as the size of the remaining jumps tends to zero. The discarded random jumps are all of the form $r^B v$ where $v \in S_B$ and $r \le \epsilon$. If B has no nilpotent part then $\|r^B v\|_B \le \epsilon^{b_*}$. Hence in order to retain all jumps larger than m it suffices to take $\epsilon = m^{1/b_*}$, and then the number of jumps simulated will be Poisson with mean $m^{-1/b_*}T\lambda(S_B)$. If there is a nilpotent part, the bound involves additional $\log\epsilon$ terms. The approximation converges faster, as $\epsilon \to 0$, when the real parts of the eigenvalues of B are uniformly larger. Remark 7.2.10 in [30] shows that the exponent governs the tails of an operator stable process, and $b_* = \min\{b_1, \ldots, b_d\} > 1/2$ determines the lightest tail, in the sense that $\mathbb{E}|\langle X(t), u\rangle|^\rho$ diverges for all $\rho > 1/b_*$ and all $u \ne 0$. Hence the convergence is faster when $\mathbf{X}$ has heavier tails. In general, an operator stable process can be decomposed into two independent component processes, one Gaussian and another having no Gaussian component. The two components are supported on subspaces of $\mathbb{R}^d$ whose intersection is trivial. In practical applications, Theorem 3.1 is applied to the nonnormal component. In the case where $X(t)$ has both a normal and a nonnormal component, the resulting approximation combines a full dimensional Brownian motion with drift, and a Poissonian component restricted to the nonnormal subspace. For the remainder of this section, we will focus on simulating operator stable laws on $\mathbb{R}^2$ having no normal component.

In practical applications, it is advantageous to produce a simulated process whose mean equals that of the operator stable process $X(t)$. If every eigenvalue of the exponent B has real part $b < 1$, then the mean exists, by [30, Theorem 8.2.14]. If any eigenvalue has real part $b > 1$ then the mean is undefined. In the former case, one can choose a_ϵ so that the right-hand side in (4.1) has mean zero. Recall that the number of terms M_ϵ in the sum (3.4) defining $N^\epsilon(t)$ is Poisson with mean $\theta_\epsilon = T\lambda(S_B)/\epsilon$, and that conditional on $M_\epsilon = n$, $(\Gamma_1/\theta_\epsilon, \ldots, \Gamma_n/\theta_\epsilon)$ is equal in distribution to the vector of order statistics from n IID standard uniform random variables. Condition to get $\mathbb{E}[N^\epsilon(t)|M_\epsilon = n] = n(t/T)\mathbb{E}[(\epsilon U)^{-B}]\mathbb{E}[v]$ where U is standard uniform and v has distribution $\lambda/\lambda(S_B)$. Remove the condition and simplify to get

$$\mathbb{E}[N^\epsilon(t)] = t\lambda(S_B)\epsilon^{B-I}\mathbb{E}[U^{-B}]\mathbb{E}[v]. \tag{4.2}$$

Since $\mathbb{E}[W(t)] = 0$ we can set $a_\epsilon t = -\mathbb{E}[N^\epsilon(t)]$ to get mean zero. Note that for such B we have $\|\epsilon^{B-I}x\| \to \infty$ for all $x \ne 0$ by [30, Theorem 2.2.4], so that $\|a_\epsilon\| \to \infty$ as $\epsilon \to 0$. This reflects the fact that, in the finite mean case, the infinite series (3.1) does not converge without centering. Finally we note that, if $\mathbb{E}[v] = 0$, then no centering is necessary.

In this section, we assume a fixed coordinate system on $\mathbb{R}^2$ with the standard coordinate vectors $e_1 = [1, 0]^\top$ and $e_2 = [0, 1]^\top$, and we write $X(t) = X_1(t)e_1 + X_2(t)e_2$. Recall that a strictly operator stable process satisfies the scaling relationship

$$X(t) \stackrel{d}{=} t^B X(1) \tag{4.3}$$

for all $t > 0$. All plots in this section use $T = 1$ and $\epsilon = 0.001$, and we show the simulated processes at the time points $t = n\Delta t$ for $0 \le t \le T$ with $\Delta t = 0.001$. Unless otherwise noted, we use the standard Euclidean norm. Computer codes are available from the authors.

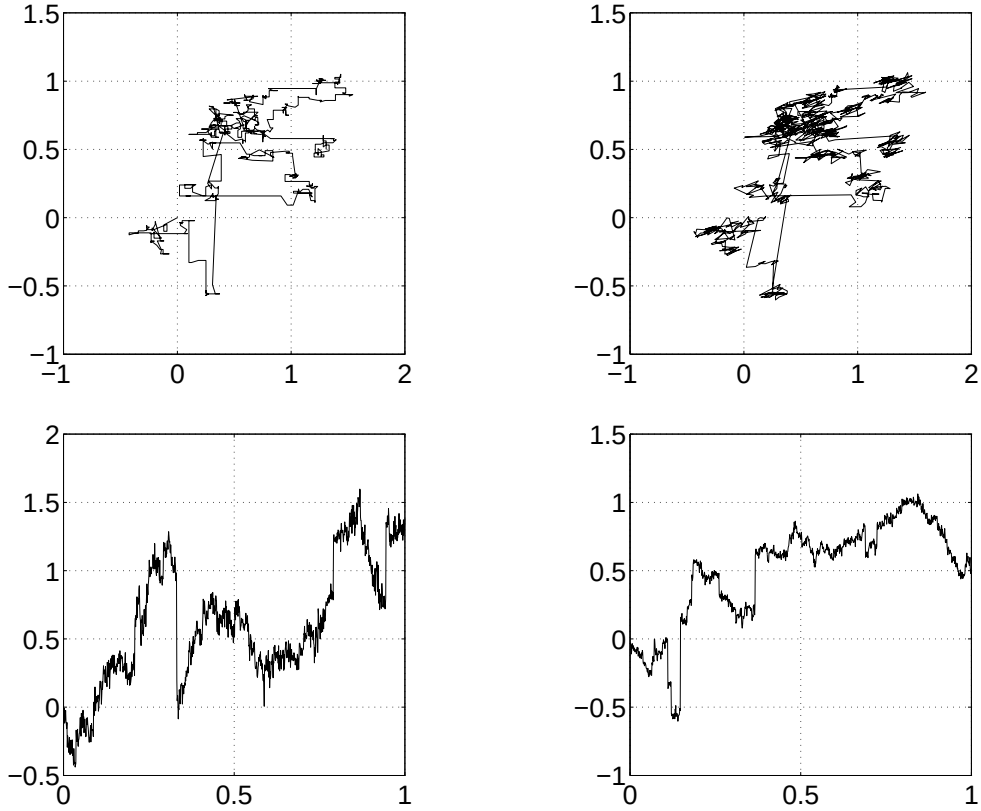

FIGURE 1. Simulated operator stable process for Example 4.1, with a diagonal exponent and a discrete spectral measure. Top left panel shows the sample path of the shot noise process $N^\epsilon(t)$, and top right panel shows the corresponding operator stable process $X(t)$. Bottom left panel shows the marginal process $X_1(t)$, and bottom right panel shows $X_2(t)$.

Example 4.1. This simple example has a diagonal exponent and a discrete spectral measure. Equation (4.1) was used to simulate an operator stable process $X(t)$ whose exponent is diagonal

$$B = \begin{bmatrix} 1/1.8 & 0 \\ 0 & 1/1.5 \end{bmatrix} = \mathrm{diag}(b_1, b_2)$$

so that $Be_i = b_i e_i$ with $b_1 = 1/1.8$ and $b_2 = 1/1.5$. Were we to take $b_2 = b_1$, this would be a stable process. Since the exponent is already in Jordan form, we can take $\|x\|_B$ to be the usual Euclidean norm, so that S_B is the unit circle. We choose the spectral measure λ to place equal masses of $1/4$ at the four points $\pm e_1$ and $\pm e_2$. Then $\mathbb{E}[v] = 0$ in (4.2) so that no centering is needed, as the simulated process has mean zero without any centering. Then $\Lambda = \mathrm{diag}(1/2, 1/2)$, $\Sigma_1 = \mathrm{diag}(9/2, 3/2)$, and $A_\epsilon = \mathrm{diag}(3\sqrt{5}\sqrt[3]{10}/10, \sqrt{15}/10)$. It is easy to see from the definition $t^B = I + B\log t + (B\log t)^2/2! + \cdots$ that $t^B = \mathrm{diag}(t^{b_1}, t^{b_2})$. From the scaling relation (4.3) it follows that

$$X_i(t) \stackrel{d}{=} t^{b_i} X_i(1).$$

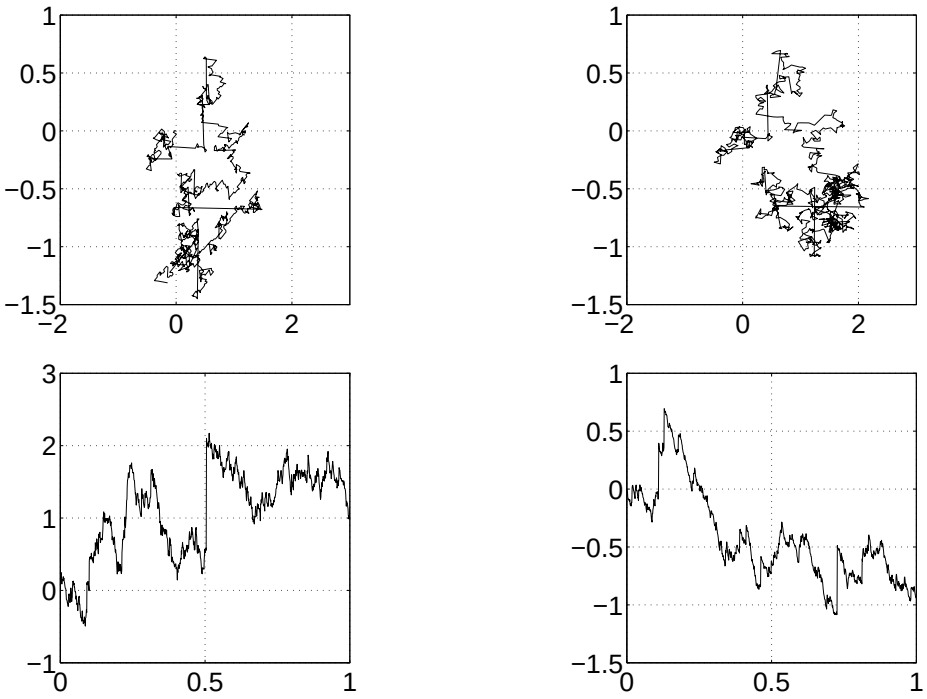

FIGURE 2. Simulated operator stable process for Example 4.2, with independent skewed stable marginals. Top left panel shows the sample path of the shot noise process $N^\epsilon(t)$, and top right panel shows the corresponding operator stable process $X(t)$. Bottom panels show the marginal processes $X_1(t)$ and $X_2(t)$.

Hence the coordinate marginals are (strictly) stable with index $\alpha_1 = 1/b_1 = 1.8$ and $\alpha_2 = 1.5$, respectively. The top right panel in Figure 1 shows a typical sample path of the process, an irregular meandering curve punctuated by occasional large jumps. The top left panel shows the corresponding shot noise part $N^\epsilon(t)$ before the Gaussian approximation of the small jumps is added. Since the spectral measure is concentrated on the coordinate axes, the large jumps are all either horizontal or vertical. Pruitt and Taylor [40] showed that the Hausdorff dimension of the sample path is $\max\{\alpha_1, \alpha_2\} = 1.8$ with probability one. A comparison of the two top panels in Figure 1 shows the importance of small jumps for the "roughness" of the sample paths, which is the practical meaning of the Hausdorff dimension. The bottom panels in Figure 1 graph each marginal process. Lemma 2.3 in Meerschaert and Scheffler [29] shows that these coordinate marginals $X_1(t)$ and $X_2(t)$ are independent stable processes. Note that the large jumps occur at different times, reflecting the independence of the marginals. Blumenthal and Getoor [6] showed that the graph of the stable process $X_i(t)$ has Hausdorff dimension $2 - 1/\alpha_i$. The bottom left graph is "rougher" due to its higher dimension. Modifying the spectral measure in this example can introduce skewness, and/or dependence between the marginals.

Example 4.2. The same exponent B is used as in Example 4.1, but now we take the spectral measure $\lambda(e_i) = 1/2$. The matrices Λ and A_ϵ turn out to be the same as Example

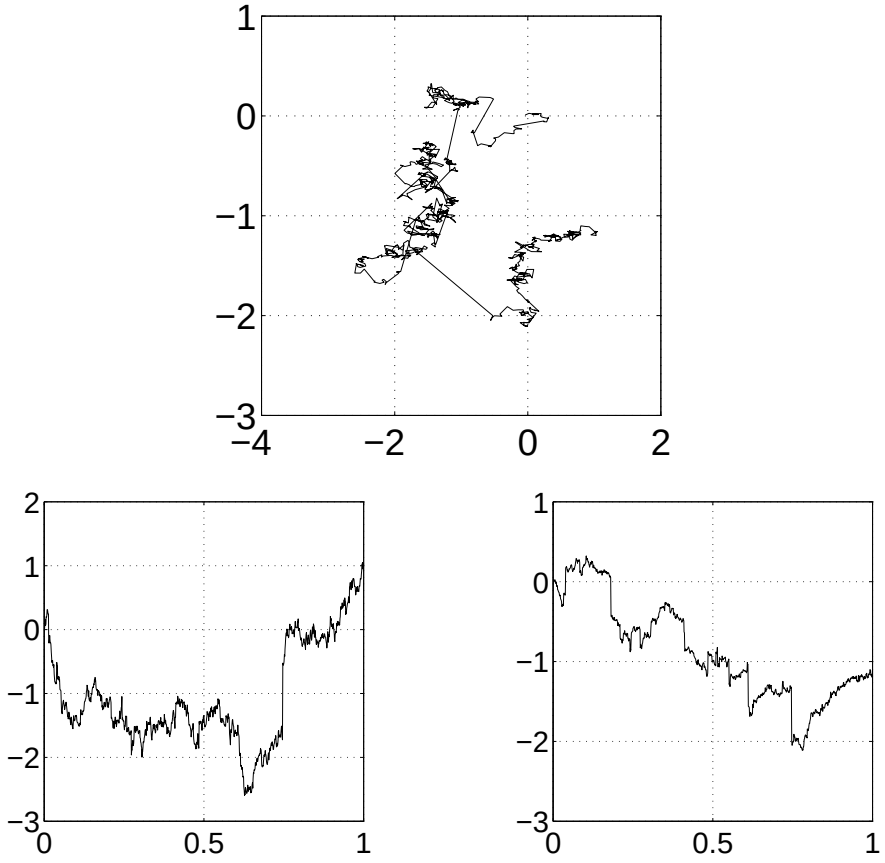

FIGURE 3. Simulated operator stable process for Example 4.3, with a diagonal exponent and a continuous spectral measure. Top panel shows the sample path of the operator stable process. Bottom panels show the marginal processes.

4.1. The marginals $X_i(t)$ are still stable with index $\alpha_1 = 1.8$ and $\alpha_2 = 1.5$, but they are no longer symmetric, and we center to zero expectation. From (4.2) we get $a_\epsilon = [45\sqrt[3]{10}/4, 15]^\top$ to compensate the shot noise portion to mean zero. Figure 2 shows a typical sample path and component graphs for this process. Since the spectral measure is concentrated on the positive coordinate axes, the large jumps apparent in the component graphs are all positive.

Example 4.3. This example illustrates the effect of a continuous spectral measure. We use the same exponent B as in Example 4.1, but now we take the spectral measure λ to be uniformly distributed on the unit circle: set $v = (x^2 + y^2)^{-1/2}[x, y]^\top$ where x, y are independent standard normal. The matrices Λ and A_ϵ turn out to be the same as Example 4.1. Since $\mathbb{E}[v] = 0$, no centering is needed. The marginals $X_i(t)$ are symmetric stable with index $\alpha_1 = 1.8$ and $\alpha_2 = 1.5$, but they are no longer independent. The top panel in Figure 3 shows a typical sample path of the process. Since the spectral measure is uniform, the large jumps apparent in the sample path take a random orientation. Theorem 3.2 in

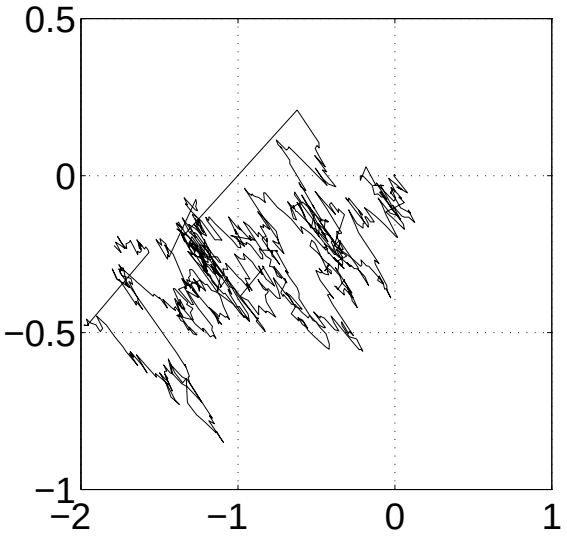

FIGURE 4. Simulated operator stable sample path for Example 4.4, a model of contaminant transport in fractured rock. The exponent has two distinct real eigenvalues, and the discrete spectral measure is concentrated on the eigenvector coordinates.

Meerschaert and Xiao [34] shows that the sample path is a random fractal, a set whose Hausdorff and packing dimension are both equal to 1.8 with probability one. The bottom panels in Figure 3 show the graphs of each marginal process. Note that the large jumps in both marginals are simultaneous, reflecting the dependence. An asymmetric continuous spectral measure can represent preferential directions for large jumps, see Reeves et al. [43, Section 3.5] for an illustration.

Example 4.4. Figure 2 of Zhang et al. [51] represents a model of contaminant transport in fractured rock. Pollution particles travel along fractures in the rock, which form at specific angles due to the geological structure of the rock matrix. An operator stable process $X(t)$ represents the path of a pollution particle, with independent skewed stable components in the fracture directions. The skewness derives from the fact that particles jump forward (downstream) when mobilized by water that flows through the fractured rock. The two components of $X(t)$ are skewed stable with index $\alpha = 1.3$ on the line with angle $\theta_1 = 30°$ measured from the positive e_1 axes as usual, and index 1.7 on the line with angle $\theta_2 = -35°$. The e_1 axis represents the overall direction of flow, caused by a differential in hydraulic head (pressure caused by water depth). The exponent B has one eigenvalue $b_1 = 1/1.3$ with associated eigenvector $v_1 = R_{\theta_1} e_1 = [.865, .500]^\top$, and another eigenvalue $b_2 = 1/1.7$ with associated eigenvector $v_2 = R_{\theta_2} e_1 = [.820, -.572]^\top$. The spectral measure is specified as $\lambda(v_1) = 0.4$ and $\lambda(v_2) = 0.6$, representing the relative fraction of jumps along each fracture direction. In order to compute the matrix power t^B

a change of basis is useful. Define the matrix P according to $Pe_i = v_i$ so that

$$P = \begin{bmatrix} .865 & .820 \\ .500 & -.572 \end{bmatrix}$$

and $D = P^{-1}BP = \mathrm{diag}(b_1, b_2)$ is a diagonal matrix. Then the exponent

$$B = PDP^{-1} = \begin{bmatrix} .688 & .142 \\ .057 & .671 \end{bmatrix}.$$

From (3.9) we get

$$\Lambda = \begin{bmatrix} .703 & -.109 \\ -.109 & .297 \end{bmatrix}.$$

Since $t^D = \mathrm{diag}(t^{b_1}, t^{b_2})$ we can compute $t^B = Pt^DP^{-1}$ and integrate in (3.8) to get the Gaussian covariance matrix Σ_ϵ whose symmetric square root is given by

$$A_\epsilon = \begin{bmatrix} 0.723 & -0.416 \\ -0.416 & 0.407 \end{bmatrix}$$

To compute the square root, we decompose $\Sigma_\epsilon = QEQ^{-1}$ where $E = \mathrm{diag}(c_1, c_2)$, c_i are the eigenvalues of Σ_ϵ, and the columns of Q are the corresponding eigenvectors, so that $A_\epsilon = QE^{1/2}Q^{-1}$ where $E^{1/2} = \mathrm{diag}(c_1^{1/2}, c_2^{1/2})$. From (4.2) we get $a_\epsilon = [27.9, -10.1]^\top$ to compensate the shot noise portion to mean zero. Note that $B^\top u_i = b_i u_i$ where $u_1 = [.572, .820]^\top$ and $u_2 = [.500, -.865]^\top$ are the dual basis vectors. Then each projection $\langle X(t), u_i\rangle$ is (strictly) stable with index $\alpha_i = 1/b_i$, since

$$\langle X(t), u_i\rangle \stackrel{d}{=} \langle t^B X(1), u_i\rangle = \langle X(1), t^{B^\top} u_i\rangle = \langle X(1), t^{b_i} u_i\rangle = t^{b_i}\langle X(1), u_i\rangle.$$

Hence $.572X_1(t) + .820X_2(t)$ is stable with index $\alpha_1 = 1.3$ and $.500X_1(t) - .865X_2(t)$ is stable with index $\alpha_2 = 1.7$. Lemma 2.3 in [29] shows that these two skewed stable processes are independent, since the spectral measure is concentrated on the eigenvector coordinate axes $\langle x, v_i\rangle = 0$. The sample path in Figure 4 illustrates the dispersion of a typical pollution particle away from the center of mass of the contaminant plume. Dispersion is the spreading of particles due to variations in velocity, and it is the main cause of plume spreading in ground water hydrology. In this application, the mean zero operator stable process $X(t)$ represents particle location in a moving coordinate system, with origin at the plume center of mass. Note that the large jumps lie in the fracture directions v_i. The coordinate marginals $X_i(t)$ in this example are not stable, and they are not independent. Variations on this example are discussed in Zhang et al. [51] and Reeves et al. [43], in which the spectral measure is modified to code different flow geometries.

Example 4.5. We simulate an operator stable process $X(t)$ whose exponent has a nilpotent part

$$B = \begin{bmatrix} 1/1.5 & 0 \\ q & 1/1.5 \end{bmatrix}$$

for some $q > 0$. Note that if $q = 0$ this reduces to a stable process with index $\alpha = 1.5$. We choose the spectral measure λ to place equal masses of $1/4$ at the four points $\pm e_1$ and $\pm e_2$. Then $\mathbb{E}[v] = 0$ in (4.2) so that no centering is needed. Here $\Lambda = \mathrm{diag}(1/2, 1/2)$,

$$\Sigma_1 = \begin{bmatrix} 3/2 & -9q/2 \\ -9q/2 & (3 + 54q^2)/2 \end{bmatrix}$$

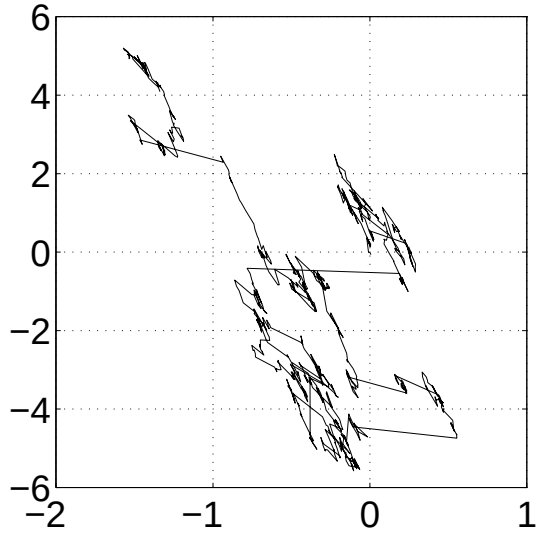

FIGURE 5. Simulated operator stable sample path for Example 4.5. The exponent has a nilpotent part, and the discrete spectral measure is concentrated on the coordinate axes.

and, in the case $q = 1$,

$$A_\epsilon = \begin{bmatrix} 0.146 & -0.359 \\ -0.359 & 4.009 \end{bmatrix}.$$

Note that $t^B = t^b t^N$ where $b = 1/1.5$ and

$$t^N = \begin{bmatrix} 1 & 0 \\ q \log t & 1 \end{bmatrix}.$$

From (4.3) it follows that the second marginal $X_2(t)$ is symmetric stable with index $\alpha = 1/b = 1.5$. The first marginal is not stable, but it lies in the domain of attraction of a symmetric stable with index $\alpha = 1.5$, see [27, Theorem 2]. Figure 5 shows a typical sample path of the process in the case $q = 1$. The large jumps apparent in the sample path of Figure 5 are all of the form $t^B v$ where $v = \pm e_i$ and $t > 0$. Hence they are either vertical, or they lie on the curved orbits $\pm t^B e_1$. Theorem 3.2 in [34] shows that the sample path is almost surely a random fractal with dimension 1.5. Lemma 2.3 in [29] shows that the coordinates $X_1(t)$ and $X_2(t)$ are not independent.

Example 4.6. We simulate an operator stable process $X(t)$ whose exponent

$$B = \begin{bmatrix} 1/1.5 & 1 \\ -1 & 1/1.5 \end{bmatrix}$$

has complex eigenvalues $b \pm i$ with $b = 1/1.5$. We choose the spectral measure λ to place equal masses of $1/4$ at the four points $\pm e_1$ and $\pm e_2$, so that $\mathbb{E}[v] = 0$ in (4.2) and no

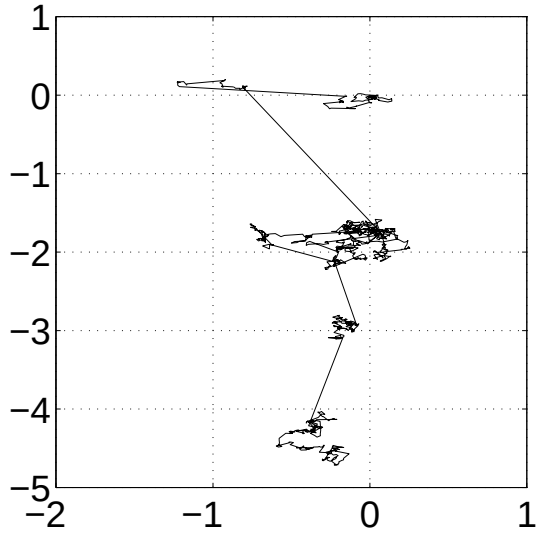

FIGURE 6. Simulated operator stable sample path for Example 4.6, whose exponent has complex eigenvalues.

centering is needed. Here $\Lambda = \mathrm{diag}(1/2, 1/2)$, and

$$A_\epsilon = \begin{bmatrix} 0.387 & 0.0 \\ 0.0 & 0.387 \end{bmatrix}.$$

In this case, $t^B = t^b R_{\theta(t)}$ with $\theta(t) = \ln t$, since we can write $B = bI + K$ where the matrix exponential $\exp(sK) = R_s$. The coordinate marginals $X_1(t)$ and $X_2(t)$ are not stable, but they are both semistable with index $\alpha = 1/b = 1.5$, see [27, Theorem 2]. Lemma 2.3 in [29] shows they are not independent. Figure 6 shows a typical sample path of the process. The large random jumps are of the form $t^B v$ where $v = \pm e_i$, so that the angle varies along with the length of the jump. The sample path is a fractal with dimension 1.5, see [34, Theorem 3.2].

Example 4.7. Figure 1 in Zhang et al. [51] presents an operator stable model $X(t)$ with diagonal exponent

$$B = \begin{bmatrix} 1/1.5 & 0 \\ 0 & 1/1.9 \end{bmatrix}$$

and spectral measure λ that places masses of 0.3 at e_1, 0.2 at $\pm 6°$, 0.1 at $\pm 12°$, and 0.05 at $\pm 18°$ on the unit sphere in the standard Euclidean norm. Large jumps are along the positive x-axis, or along the orbits $t^B u$ where u is a unit vector at $\pm 6°$, $\pm 12°$, or $\pm 18°$, representing displacements of a pollutant particle in an underground aquifer with a mean flow in the positive x direction, but some dispersion due to the intervening porous medium. The average plume velocity is $v = [10, 0]^\top$ so that $\mathbb{E}[X(t)] = tv$. Figure 7 depicts the path of a typical particle. Here

$$\Lambda = \begin{bmatrix} 0.977 & 0.0 \\ 0.0 & 0.0226 \end{bmatrix}$$

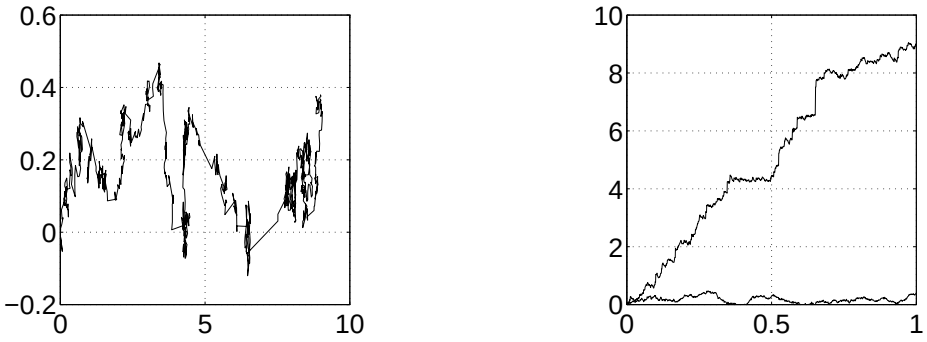

FIGURE 7. Simulated operator stable process for Example 4.7, modeling a pollution particle moving through underground water in a heterogeneous porous medium consisting of sand, gravel, and clay. Left panel depicts the sample path of a moving particle. Right panel shows the coordinate marginals.

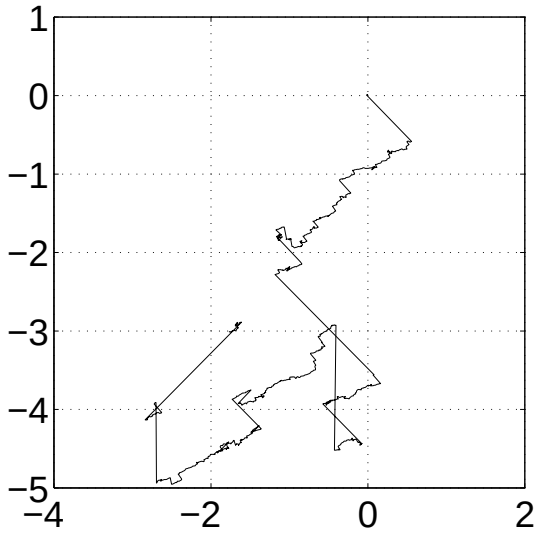

FIGURE 8. Simulated operator stable sample path for Example 4.8, modeling the motion of a pollution particle moving through water in fractured rock. The mean zero sample path represents deviation from the plume center of mass.

and

$$A_\epsilon = \begin{bmatrix} 0.541 & 0.0 \\ 0.0 & 0.546 \end{bmatrix}.$$

From (4.2) we compute $a_\epsilon = [29.7, 0]^\top$ and, in the simulation code, we first center to mean zero, and then add the mean velocity.

Example 4.8. This example follows the transport model number 22 for contaminant transport in complex fracture networks from Reeves et al. [43]. The exponent B has eigenvectors $v_1 = [\sqrt{2}/2, \sqrt{2}/2]^\top$ and $v_2 = [\sqrt{2}/2, -\sqrt{2}/2]^\top$ at $+45°$ and $-45°$ on the unit circle with eigenvalues $b_1 = 1/1.1$ and $b_2 = 1/1.2$ respectively. Writing $Pe_i = v_i$ we get $D = P^{-1}BP = \mathrm{diag}(b_1, b_2)$ so that

$$B = PDP^{-1} = \begin{bmatrix} 115/132 & 5/132 \\ 5/132 & 115/132 \end{bmatrix}$$

Since $t^D = \mathrm{diag}(t^{b_1}, t^{b_2})$ we also have

$$t^B = Pt^DP^{-1} = \begin{bmatrix} (t^{b_1} + t^{b_2})/2 & (t^{b_1} - t^{b_2})/2 \\ (t^{b_1} - t^{b_2})/2 & (t^{b_1} + t^{b_2})/2 \end{bmatrix}$$

The spectral measure has weights 0.4 and $\pm 45°$ and 0.2 at e_2. The Lévy measure is concentrated on the two straight line orbits $\{t^B v_i : t > 0\}$ and on the curved orbit $\{t^B e_2 : t > 0\}$. Marginals $\langle X(t), v_i \rangle$ are stable with index $\alpha_1 = 1.1$ and $\alpha_2 = 1.2$ respectively, but they are not independent, since the spectral measure is not concentrated on the eigenvector axes. The first marginal process $\langle X(t), v_1 \rangle$ is positively skewed, since the projection of the Lévy measure onto the first eigenvector coordinate places all mass on the positive half line. The second marginal $\langle X(t), v_2 \rangle$ is the sum of two independent stable processes, one with positive skewness resulting from the v_2 orbit, and one with negative skewness resulting from the projection of the e_2 orbit onto the negative v_2 axis. As in Example 4.4 we compute $\Lambda = \mathrm{diag}(0.4, 0.6)$ and

$$A_\epsilon = \begin{bmatrix} 0.0603 & -0.0204 \\ -0.0203 & 0.0723 \end{bmatrix}.$$

From (4.2) we compute $a_\epsilon = [11.35, 4.43]^\top$ to correct the shot noise process to mean zero. Figure 8 shows a typical sample path. In this case, the sample path represents the growing deviation of a typical pollution particle from the plume center of mass.

Example 4.9. This example illustrates computation of the norm (2.3) when the exponent is not in Jordan form. The matrix

$$B = \begin{bmatrix} 1/1.8 & 1/2 \\ 0 & 1/1.5 \end{bmatrix}$$

has eigenvalue-eigenvector pairs $Bv_i = b_i v_i$ with $b_1 = 1/1.8$, $v_1 = e_1$, $b_2 = 1/1.5$, and $v_2 = (9/2)e_1 + e_2$. In order to compute the matrix power t^B it is advantageous to write the Jordan form. The matrix B has eigenvalue-eigenvector pairs $Bv_i = b_i v_i$ with $b_1 = 1/1.8$, $v_1 = [1, 0]^\top = e_1$, $b_2 = 1/1.5$, and $v_2 = [9/2, 1]^\top = (9/2)e_1 + e_2$ so that a change of basis is useful. Define the matrix P according to $Pe_i = v_i$ so that

$$P := \begin{bmatrix} 1 & 9/2 \\ 0 & 1 \end{bmatrix} \quad \text{and} \quad P^{-1} = \begin{bmatrix} 1 & -9/2 \\ 0 & 1 \end{bmatrix}$$

so that

$$D := P^{-1}BP = \begin{bmatrix} 1/1.8 & 0 \\ 0 & 1/1.5 \end{bmatrix}$$

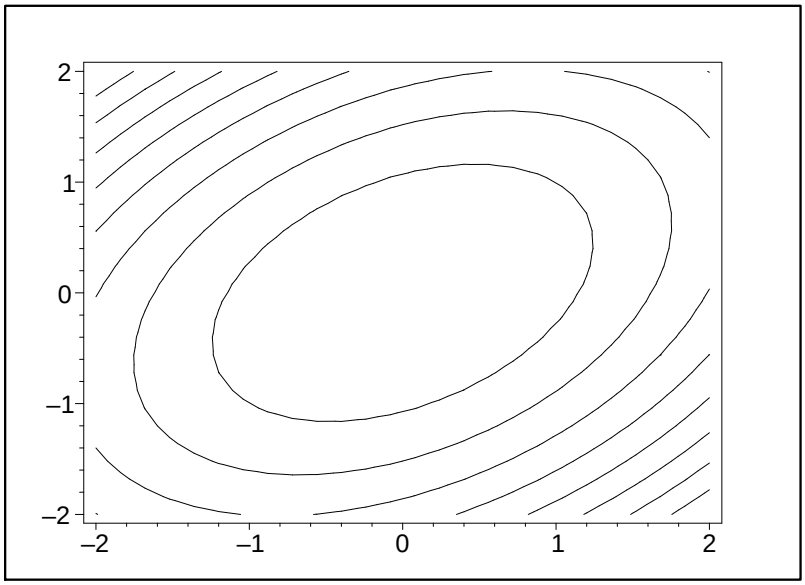

FIGURE 9. Level sets of the norm $\|x\|_B$ used in example 4.9.

is a diagonal matrix. Then

$$t^D = \begin{bmatrix} t^{1/1.8} & 0 \\ 0 & t^{1/1.5} \end{bmatrix}$$

and since $B = PDP^{-1}$ to follows from the definition $t^B = I + B + B^2/2! + \cdots$ that

$$t^B = \begin{bmatrix} t^{1/1.8} & -(9/2)t^{1/1.8} + (9/2)t^{1/1.5} \\ 0 & t^{1/1.5} \end{bmatrix}$$

We compute the norm (2.3) with $p = 2$: $\|x\|_B^2 = (9/10)x_1^2 - (81/110)x_1x_2 + (903/880)x_2^2$ so that the unit sphere S_B is an ellipse, whose major axis is rotated approximately 50° counterclockwise from the e_1 direction. Figure 9 shows level sets of this norm. The spectral measure λ places equal masses of $1/4$ at each point where the unit sphere S_B intersects the coordinate axes: $\pm c_i e_i$ where $c_1^2 = 10/9$ and $c_2^2 = 880/903$. Here $\Lambda = \mathrm{diag}(5/9, 440/903)$, and

$$A_\epsilon = \begin{bmatrix} 5.209 & -0.266 \\ -0.266 & 0.274 \end{bmatrix}.$$

The second coordinate $X_2(t)$ is symmetric stable with index $\alpha_2 = 1.5$, and the projection onto the remaining eigenvector $X_1(t) - (9/2)X_2(t)$ is stable with index $\alpha_1 = 1.8$. These two stable marginals of $X(t)$ are not independent, since the spectral measure is not concentrated on the eigenvector axes. Figure 10 shows a typical sample path for this process. The large jumps of the process are all of the form $t^B v$ where $v = \pm c_1 e_1$ or $v = \pm c_2 e_2$, since we have concentrated the spectral measure at these points. If $v = \pm c_1 e_1$ then, since e_1 is an eigenvector of B (and hence of t^B), these jumps will be in the horizontal. The remaining jumps lie along the orbits $\{\pm t^B c_2 e_2 : t > 0\}$. Any exponent, with any coordinate system and norm, can be accommodated in an operator stable model, but an exponent in Jordan form and Euclidean geometry is the most straightforward.

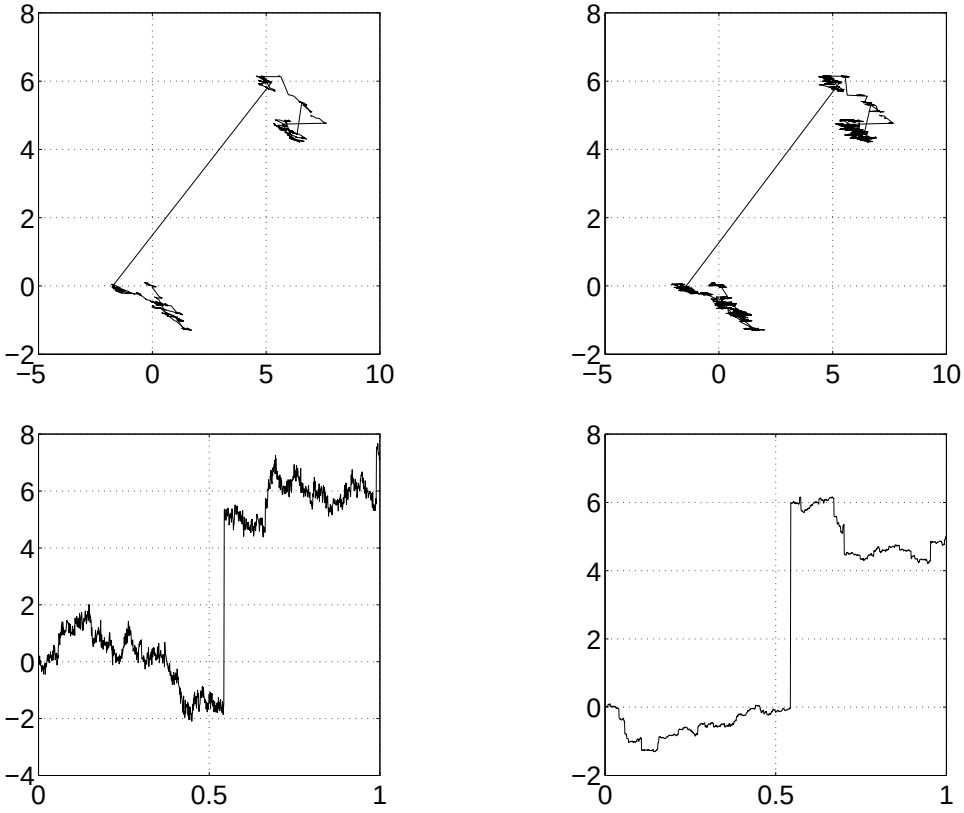

FIGURE 10. Operator stable sample path for example 4.9, whose exponent B is not given in Jordan form.

5. Exponents and Symmetries in two dimensions

The examples in Section 4 illustrate the wide range of sample path behavior for an operator stable Lévy process $\mathbf{X}$ in $\mathbb{R}^2$ with exponent B and spectral measure λ. In this section, we consider the important modeling issue of symmetry in the distribution of $X(t)$. First we classify the possible symmetries in two dimensions, in terms of the exponent. For any operator stable law, a change of coordinates puts the exponent into Jordan form. Theorem 5.1 shows that all symmetries are orthogonal in this coordinate system, and then describes the possible symmetries for each exponent. Theorem 5.2 shows how the exponent and spectral measure interact to determine the symmetries. In short, the exponent B determines the orbits t^B and, if these orbits are curved, it can break the symmetry in the spectral measure. Finally Remark 5.3 shows how to explicitly construct a process $\mathbf{X}$ with any given exponent and any admissible symmetry group, by selecting the appropriate spectral measure. Symmetry is an important modeling consideration, and a useful guide to model selection. In many practical applications, the natural symmetries of the system are known, and these results can be used to calibrate the choice of parameters.

For any full dimensional probability distribution μ, the set of symmetries

$$\mathcal{S}(\mu) := \left\{ A \in \mathrm{GL}(\mathbb{R}^d) : \; A\mu = \mu * \delta_x \text{ for some } x \in \mathbb{R}^d \right\} \tag{5.1}$$

forms a compact subgroup of $\mathrm{GL}(\mathbb{R}^d)$, see for example [5]. If the full operator stable law $\mu = \mathcal{L}(X(1))$ has a large degree of symmetry, the exponent B in (1.2) is not unique. The possible exponents are given by [17, Theorem 4.6.7]:

$$\mathcal{E}(\mu) = B + T\mathcal{S}(\mu) \tag{5.2}$$

where $B \in \mathcal{E}(\mu)$ is arbitrary. Here $T\mathcal{S}(\mu)$ is the tangent space of $\mathcal{S}(\mu)$ at the identity. If $\mathcal{S}(\mu)$ is finite, then $T\mathcal{S}(\mu) = \{0\}$, and the exponent is unique. If $A \in \mathcal{S}(\mu)$ and B is an exponent of μ, then so is $A^{-1}BA$. When the exponent is unique, we must have $AB = BA$, so B commutes with $\mathcal{S}(\mu)$. The use of commuting exponents simplifies the analysis of $\mathcal{E}(\mu)$. Every operator stable law μ has an exponent B_c that commutes with $\mathcal{S}(\mu)$, see [17, Theorem 4.7.1]. If μ is operator stable with $\mathcal{S}(\mu) = \mathcal{O}_d$, the orthogonal group on $\mathbb{R}^d$, then $B_c = \beta I$ for some $\beta > 0$ is the only commuting exponent, and μ is multivariable stable with index $1/\beta$. Since $T(\mathcal{O}_d) = \mathcal{Q}_d$ is the linear space of skew symmetric matrices, we get from (5.2) that

$$\mathcal{E}(\mu) = \beta I + \mathcal{Q}_d. \tag{5.3}$$

Recall that a matrix Q is skew-symmetric if $Q^\top = -Q$, where $Q^\top$ is the transpose of Q. If $\mathcal{S}(\mu)$ is an arbitrary compact subgroup of $\mathrm{GL}(\mathbb{R}^d)$, then by a classical result of algebra (see, e.g., [5, Theorem 5]) there exists a symmetric positive-definite matrix W and a compact subgroup $\mathcal{G}$ of the orthogonal group $\mathcal{O}_d$ such that

$$\mathcal{S}(\mu) = W^{-1}\mathcal{G}W. \tag{5.4}$$

Then (5.2) becomes

$$\mathcal{E}(\mu) = B + W^{-1}\mathcal{H}W, \tag{5.5}$$

where $\mathcal{H}$ is the tangent space of $\mathcal{G}$.

Theorem 2 in [28] implies that a compact subgroup $\mathcal{G}$ of $\mathrm{GL}(\mathbb{R}^d)$ can be the symmetry group of a full dimensional probability distribution on $\mathbb{R}^d$ if and only if it is maximal, meaning that $\mathcal{G}$ cannot be strictly contained in any other subgroup that has the same orbits. For example, the special orthogonal group $\mathcal{O}_d^+$ is not maximal because $\mathcal{O}_d^+ x = \mathcal{O}_d x$ for every $x \in \mathbb{R}^d$, and $\mathcal{O}_d^+$ is a proper subgroup of $\mathcal{O}_d$. Consequently, $\mathcal{O}_d^+$ cannot be the symmetry group of any full dimensional probability measure on $\mathbb{R}^d$. Actually Theorem 2 in [28] characterizes the strict symmetry group of μ defined by

$$\mathcal{S}_0(\mu) := \big\{A \in \mathrm{GL}(\mathbb{R}^d) : \, A\mu = \mu\big\}. \tag{5.6}$$

However, Theorem 5 in Billingsley [5] implies that $\mathcal{S}(\mu) = \mathcal{S}_0(\mu * \delta_a)$ for some $a \in \mathbb{R}^d$. Hence $\mathcal{S}(\mu)$ must be maximal as well. Moreover, we have a relation between the symmetries of μ and the strict symmetries of the Lévy measure ν in (2.2):

$$\mathcal{S}(\mu) = \mathcal{S}_0(\nu) := \big\{A \in \mathrm{GL}(\mathbb{R}^d) : \, A\nu = \nu\big\}, \tag{5.7}$$

which is valid for any infinitely divisible distribution without Gaussian part.

Since the real parts of the eigenvalues of B are greater than $1/2$, there is a coordinate system in which the exponent assumes one the following Jordan forms

$$B_0 = bI, \quad B_1 = \begin{bmatrix} b_1 & 0 \\ 0 & b_2 \end{bmatrix}, \quad B_2 = \begin{bmatrix} b & -c \\ c & b \end{bmatrix}, \quad B_3 = \begin{bmatrix} b & 0 \\ 1 & b \end{bmatrix} \tag{5.8}$$

where $b, b_1, b_2 > 1/2$, $b_1 \neq b_2$, and $c \neq 0$. If $B = B_0$, then $\mathbf{X}$ is a multivariable stable process with index $\alpha = 1/b$, and all maximal compact subgroups of $\mathrm{GL}(\mathbb{R}^2)$ are admissible

as $\mathcal{S}(\mu)$. A genuine operator stable Lévy process is obtained when $B = B_i$, $i = 1, 2, 3$. Our first question is, what are possible symmetry groups?

To deal with this question, we need to review some basic facts about subgroups of the orthogonal group $\mathcal{O}_2$ on $\mathbb{R}^2$, which can be found, e.g, in [3]. Recall that $\mathcal{O}_2$ consists of rotations and reflections,

$$\mathcal{O}_2 = \{R_\theta, F_\theta : \theta \in [0, 2\pi)\},$$

where

$$R_\theta = \begin{bmatrix} \cos\theta & -\sin\theta \\ \sin\theta & \cos\theta \end{bmatrix} \quad \text{and} \quad F_\theta = \begin{bmatrix} \cos\theta & \sin\theta \\ \sin\theta & -\cos\theta \end{bmatrix}.$$

R_θ is a rotation counter-clockwise by θ and F_θ is a reflection through the line of angle $\theta/2$ passing through the origin. The following rules of composition hold: $R_{\theta_1} R_{\theta_2} = R_{\theta_1+\theta_2}$, $F_{\theta_1} F_{\theta_2} = R_{\theta_1-\theta_2}$, $R_{\theta_1} F_{\theta_2} = F_{\theta_1+\theta_2}$, $F_{\theta_2} R_{\theta_1} = F_{\theta_2-\theta_1}$.

The group of rotations $\mathcal{O}_2^+ = \{R_\theta : \theta \in [0, 2\pi)\}$ is the only infinite proper compact subgroup of $\mathcal{O}_2$. There are also only two kinds of finite subgroups of $\mathcal{O}_2$ (modulo the orthogonal conjugacy, see [3, Ch. VII.3]):

(1) Cyclic group $\mathcal{C}_n = \{R_{k2\pi/n} : k = 0, \ldots, n-1\}$, $n \geq 1$,
(2) Dihedral group $\mathcal{D}_n = \{R_{k2\pi/n}, F_{k2\pi/n} : k = 0, \ldots, n-1\}$, $n \geq 1$.

Notice that $\mathcal{C}_1 = \{I\}$, $\mathcal{C}_2 = \{I, -I\}$, $\mathcal{D}_1 = \{I, F_0\}$, and $\mathcal{D}_2 = \{I, F_0, -I, -F_0\}$, where

$$F_0 = \begin{bmatrix} 1 & 0 \\ 0 & -1 \end{bmatrix}$$

is the reflection with respect to the x-axis. We will also need $\mathcal{D}_1^* = \{I, -F_0\}$, the group of reflection with respect to the y-axis, which is orthogonally conjugate to $\mathcal{D}_1$.

The next result characterizes the possible symmetries of the distribution of $X(t)$ in the truly operator stable case where $B = B_i$ in (5.8) for some $i = 1, 2, 3$. In view of (2.1), the symmetry group do not depend on t. Remarkably, once the exponent takes the Jordan form, all symmetries must be orthogonal.

Theorem 5.1. *Let $\mathbf{X} = \{X(t)\}_{t\geq 0}$ be a full operator stable Lévy processes on $\mathbb{R}^2$ with an exponent B in the Jordan form (5.8), and let $\mu = \mathcal{L}(X(1))$. Then the following hold.*

(i) *If $B = B_1$, then $\mathcal{S}(\mu)$ is either $\mathcal{C}_1$, $\mathcal{C}_2$, $\mathcal{D}_1$, $\mathcal{D}_1^*$, or $\mathcal{D}_2$.*
(ii) *If $B = B_2$, then $\mathcal{S}(\mu)$ is either $\mathcal{C}_n$, $n \geq 1$, or $\mathcal{O}_2$.*
(iii) *If $B = B_3$, then $\mathcal{S}(\mu)$ is either $\mathcal{C}_1$ or $\mathcal{C}_2$.*

Proof. Suppose that μ has an exponent $B = B_i$, $i = 1, 2, 3$, and let B_c be a commuting exponent. If $\mathcal{S}(\mu)$ is finite, then $B_i = B_c$, otherwise B_c can be different from B_i. The symmetries $\mathcal{S}(\mu)$ defined in (5.1) form a compact subgroup of the centralizer $C(B_c)$,

$$\mathcal{S}(\mu) \subset C(B_c) := \{A \in \mathrm{GL}(\mathbb{R}^2) : AB_c = B_c A\}. \tag{5.9}$$

First consider finite symmetry groups $\mathcal{S}(\mu)$, so that $B_c = B_i$. If $i = 1$,

$$C(B_1) = \left\{ \begin{bmatrix} \alpha & 0 \\ 0 & \beta \end{bmatrix} : \alpha\beta \neq 0 \right\},$$

and since $\mathcal{S}(\mu)$ is finite (and thus compact),

$$\mathcal{S}(\mu) \subset \left\{ \begin{bmatrix} \alpha & 0 \\ 0 & \beta \end{bmatrix} : |\alpha| = |\beta| = 1 \right\}.$$

Thus $\mathcal{S}(\mu)$ is either $\mathcal{C}_1$, $\mathcal{C}_2$, $\mathcal{D}_1$, $\mathcal{D}_1^*$, or $\mathcal{D}_2$, as claimed. If $i = 2$, then

$$C(B_2) = \left\{ \begin{bmatrix} \alpha & -\beta \\ \beta & \alpha \end{bmatrix} : \alpha^2 + \beta^2 > 0 \right\}.$$

Since $\mathcal{S}(\mu)$ is finite (and thus compact),

$$\mathcal{S}(\mu) \subset \left\{ \begin{bmatrix} \alpha & -\beta \\ \beta & \alpha \end{bmatrix} : \alpha^2 + \beta^2 = 1 \right\},$$

so that $\mathcal{S}(\mu) = \mathcal{C}_n$, for some $n \geq 1$. If $i = 3$,

$$C(B_3) = \left\{ \begin{bmatrix} \alpha & 0 \\ \beta & \alpha \end{bmatrix} : \alpha \neq 0, \beta \in \mathbb{R} \right\},$$

and since $\mathcal{S}(\mu)$ is finite,

$$\mathcal{S}(\mu) \subset \left\{ \begin{bmatrix} \alpha & 0 \\ 0 & \alpha \end{bmatrix} : |\alpha| = 1 \right\}.$$

Thus $\mathcal{S}(\mu)$ is either $\mathcal{C}_1$ or $\mathcal{C}_2$, as claimed.

Now we consider infinite symmetry groups $\mathcal{S}(\mu)$, so that (5.4) holds. From (5.9), WB_cW^{-1} commutes with every orthogonal transformation. Thus WB_cW^{-1} is a multiple of the identity matrix, which yields

$$B_c = \beta I \tag{5.10}$$

Since $T\mathcal{O}_2 = \mathcal{Q}_2$, $B_i = B_c + W^{-1}KW = W^{-1}(\beta I + K)W$ for some skew symmetric matrix K, and so $B_i = \gamma W^{-1}R_\phi W$ for some $\gamma \neq 0$ and $\phi \in [0, 2\pi)$. This equation eliminates the cases $i = 1$ and $i = 3$ by comparing the eigenvalues on the left and right hand side. Thus $i = 2$ and $B_2 = \alpha R_\psi$ for some $\psi \in (0, \pi) \cup (\pi, 2\pi)$, from which we have

$$\alpha R_\psi = B_2 = \gamma W^{-1}R_\phi W.$$

Comparing the determinants of both sides gives $\alpha = \gamma$. Hence

$$R_\psi = W^{-1}R_\phi W.$$

Since the sets of eigenvalues of both sides of this equation must be the same, $\phi = \psi$ or $\phi = 2\pi - \psi$. If $\phi = \psi$ then $WR_\psi = R_\psi W$ for $\psi \in (0, \pi) \cup (\pi, 2\pi)$. A direct verification of this equation reveals that $W = \kappa R_\tau$ is a multiple of a rotation. (In fact, W is a scalar multiple of the identity, since it is also symmetric and positive definite.) Therefore,

$$\mathcal{S}(\mu) = (\kappa R_\tau)^{-1}\mathcal{O}_2\kappa R_\tau = \mathcal{O}_2,$$

as claimed. If $\phi = 2\pi - \psi$, then

$$R_\psi = W^{-1}R_{2\pi-\psi}W = W^{-1}F_0F_\psi W = W^{-1}F_0R_\psi F_0 W$$

or

$$(F_0W)R_\psi = R_\psi(F_0W).$$

By the same reason as above, one can verify that $F_0W = \kappa R_\tau$ is a multiple of rotation. Hence $W = \kappa F_{-\tau}$ and

$$\mathcal{S}(\mu) = (\kappa F_{-\tau})^{-1}\mathcal{O}_2\kappa F_{-\tau} = \mathcal{O}_2.$$

This proves that $B = B_2$ and $\mathcal{S}(\mu) = \mathcal{O}_2$ provided $\mathcal{S}(\mu) = W^{-1}\mathcal{O}_2W$. □

Operator stable laws are parameterized by their exponents and spectral measures. The next result shows how the interplay between the curved orbits t^B determined by the exponent, along with the symmetries of the spectral measure, combine to determine the symmetries of the process. Recall that $\mathcal{O}_2^+$ is the group of rotations.

Theorem 5.2. *Let $\mathbf{X} = \{X(t)\}_{t\geq 0}$ be a full operator stable Lévy process in $\mathbb{R}^2$ with exponent B, spectral measure λ, and no Gaussian component. Let $\mu = \mathcal{L}(X(1))$. Suppose that B is given in the Jordan form* (5.8) *and that the polar decomposition* (2.5) *holds with $S_B = S^1$, the Euclidean unit sphere of $\mathbb{R}^2$. Let $\mathcal{S}_0(\lambda) = \{A \in \mathrm{GL}(\mathbb{R}^2) : A\lambda = \lambda\}$ denote the strict symmetry group of the spectral measure.*

(a) *If $B = B_1$, then $\mathcal{S}(\mu) = \mathcal{S}_0(\lambda) \cap \mathcal{D}_2$.*
(b) *If $B = B_2$, then either $\mathcal{S}(\mu) = \mathcal{S}_0(\lambda) \cap \mathcal{O}_2^+ = \mathcal{C}_n$ for some $n \geq 1$, or $\mathcal{S}(\mu) = \mathcal{S}_0(\lambda) = \mathcal{O}_2$.*
(c) *If $B = B_3$, then $\mathcal{S}(\mu) = \mathcal{S}_0(\lambda) \cap \mathcal{C}_2$.*

Proof. Let ν be the Lévy measure of μ. Since μ does not have a Gaussian part, we have

$$\mathcal{S}(\mu) = \mathcal{S}_0(\nu) = \{A \in \mathrm{GL}(\mathbb{R}^2) : A\nu = \nu\} \tag{5.11}$$

as in (5.7). First we will show that if $B = B_i$, $i = 1, 2, 3$ and $\mathcal{S}(\mu)$ is finite, then

$$\mathcal{S}(\mu) = \mathcal{S}_0(\lambda) \cap \{A \in \mathcal{O}_2 : AB = BA\}. \tag{5.12}$$

Let $A \in \mathcal{S}(\mu)$, $\mathcal{S}(\mu)$ being finite. Then $A \in \mathcal{O}_2$ by Theorem 5.1 and A commutes with B. For every $F \in \mathcal{B}(S^1)$, $A^{-1}F \in \mathcal{B}(S^1)$ and by (2.4) and (2.5) with $S_B = S^1$ we have

$$\begin{aligned}\lambda(A^{-1}F) &= \nu(\{x : x = t^B A^{-1}v, \text{ for some } (t, v) \in [1, \infty) \times F\}) \\ &= \nu(A^{-1}\{x : x = t^B v, \text{ for some } (t, v) \in [1, \infty) \times F\}) = \lambda(F)\end{aligned}$$

because $\mathcal{S}(\mu) = \mathcal{S}_0(\nu)$ from (5.11). Hence $A \in \mathcal{S}_0(\lambda)$. The proof of the opposite inclusion in (5.12) uses similar arguments and is omitted.

Proof of (a). A direct verification shows that B_1 commutes with $\mathcal{D}_2$. Thus by (5.12)

$$\mathcal{S}_0(\lambda) \supset \mathcal{S}(\mu) \supset \mathcal{S}_0(\lambda) \cap \mathcal{D}_2.$$

Since $\mathcal{S}(\mu) \subset \mathcal{D}_2$ by Theorem 5.1, we get (a).

Proof of (b). By Theorem 5.1 $\mathcal{S}(\mu) = \mathcal{C}_n$ for some $n \geq 1$, or $\mathcal{S}(\mu) = \mathcal{O}_2$. Suppose that $\mathcal{S}(\mu) = \mathcal{C}_n$. Since $\mathcal{O}_2^+$ commutes with B_2, by (5.12) we have

$$\mathcal{S}_0(\lambda) \supset \mathcal{S}(\mu) \supset \mathcal{S}_0(\lambda) \cap \mathcal{O}_2^+.$$

Thus $\mathcal{S}(\mu) = \mathcal{S}_0(\lambda) \cap \mathcal{O}_2^+ = \mathcal{C}_n$.

Suppose $\mathcal{S}(\mu) = \mathcal{O}_2$. Then $R_\theta \in \mathcal{S}_0(\nu)$ for every θ by (5.11). Since R_θ commutes with B_2, $R_\theta \in \mathcal{S}_0(\lambda)$ by the same line of arguments as in the proof of (5.12). Hence $\mathcal{S}_0(\lambda) \supset \mathcal{O}_2^+$, which implies that λ is a finite full measure in $\mathbb{R}^2$. Then λ is a constant multiple of a probability measure, so $\mathcal{S}_0(\lambda)$ must be maximal by [28, Theorem 2], and hence $\mathcal{S}_0(\lambda) = \mathcal{O}_2$.

Proof of (c). This follows from (5.12) because $\mathcal{C}_2$ obviously commutes with B_3. □

Remark 5.3. Using Theorem 5.2 we can explicitly construct an operator stable process with any given exponent B_i for $i = 1, 2, 3$ in Jordan form (5.8) and any admissible symmetry group. For example, let λ be concentrated at four points $(\pm 2^{-1/2}, \pm 2^{-1/2})$. Choosing masses at these points appropriately, any subgroup of $\mathcal{D}_2$ is realized as $\mathcal{S}_0(\lambda)$. By Theorem

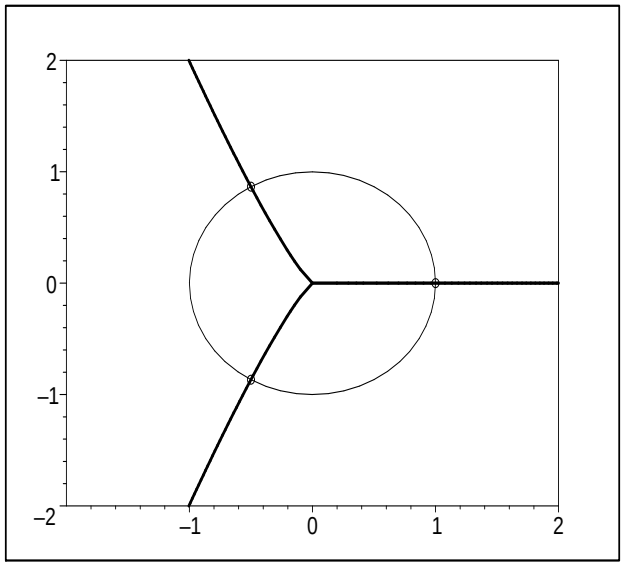

FIGURE 11. Support of the Lévy measure (thick lines) for Remark 5.4, showing the effect of the exponent B_1 on the symmetry group. The spectral measure gives equal weight to three equally spaced points on the unit circle, so that $\mathcal{S}_0(\lambda) = \mathcal{D}_3$. In this case $B = B_1$, we have $\mathcal{S}(\mu) = \mathcal{D}_1$.

5.2, all cases of $\mathcal{S}(\mu)$ are realized by this example when $B = B_1$ and $B = B_3$. When $B = B_2$, we only get $\mathcal{C}_1$ and $\mathcal{C}_2$. To get $\mathcal{S}(\mu) = \mathcal{C}_n$, $n \geq 3$, we take λ concentrated at vertices of a regular n-gon inscribed into the unit circle with one vertex at $(1, 0)$ and equal masses at all the vertices. Then $\mathcal{S}_0(\lambda) = \mathcal{D}_n$, so by Theorem 5.2, $\mathcal{S}(\mu) = \mathcal{D}_n \cap \mathcal{O}_2^+ = \mathcal{C}_n$. Finally $\mathcal{S}(\mu) = \mathcal{O}_2$ when $B = B_2$ and λ is a uniform measure on S^1.

Remark 5.4. It is interesting to see how much an exponent affects the symmetry. Consider a measure λ with $\mathcal{S}_0(\lambda) = \mathcal{D}_n$ described in Remark 5.3, with $n = 3$. Then, by Theorem 5.2, $\mathcal{S}(\mu) = \mathcal{D}_1$ when $B = B_1$, $\mathcal{S}(\mu) = \mathcal{C}_3$ when $B = B_2$, and $\mathcal{S}(\mu) = \mathcal{C}_1$ when $B = B_3$. Figure 11 illustrates the diagonal case $B = B_1$, in which the Lévy measure ν in (2.4) is symmetric with respect to reflection about the vertical axis. Here we take $b_1 = 1/1.8$ and $b_2 = 1/1.5$, but any case with $b_1 \neq b_2$ appears similar. Figure 12 illustrates the complex case $B = B_2$, where the Lévy measure is symmetric with respect to rotations that are a multiple of $2\pi/3$. Figure 13 illustrates the nilpotent case $B = B_3$, and here the Lévy measure has no nontrivial symmetries. All three cases have the same spectral measure, but a different exponent. Hence the spectral measure and the exponent are both important in determining the symmetries.

Remark 5.5. In order to tie the results of this section back to the examples in Section 4, we compute the symmetry group $\mathcal{S}(\mu)$ for each case. For Example 4.1 we have $\mathcal{S}(\mu) = \mathcal{S}_0(\lambda) = \mathcal{D}_2$ by Theorem 5.2 (a), since the exponent $B = B_1$ in (5.8), and spectral measure λ gives equal mass to the four points $\pm e_1, \pm e_2$. Example 4.2 has $\mathcal{S}(\mu) = \mathcal{C}_1$ since the spectral measure λ gives unequal mass to the two points e_1, e_2, so that Theorem 5.2 (a1) applies. The spectral measure in Example 4.3 is uniform on the unit sphere, so that $\mathcal{S}_0(\lambda) = \mathcal{O}_2$, but the symmetry is of the form $B = B_1$ in (5.8), so the symmetry group $\mathcal{S}(\mu) = \mathcal{D}_2$ by

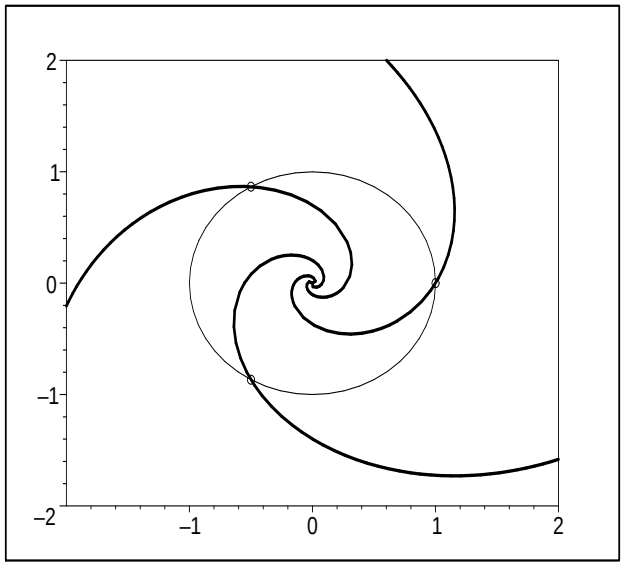

FIGURE 12. Support of the Lévy measure for Remark 5.4, showing the effect of the exponent B_2 on the symmetry group. Here $\mathcal{S}(\mu) = \mathcal{C}_3$.

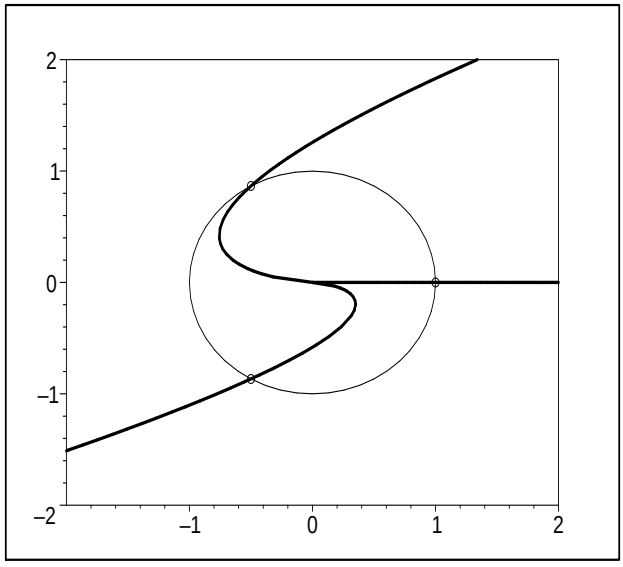

FIGURE 13. Support of the Lévy measure for Remark 5.4, showing the effect of the exponent B_3 on the symmetry group. Here $\mathcal{S}(\mu) = \mathcal{C}_1$.

Theorem 5.2 (a). For Example 4.4, note that $P^{-1}\mathbf{X}$ has exponent D of the form B_1 in (5.8). Since the spectral measure λ of $\mathbf{X}$ is concentrated on the two linear independent vectors v_1, v_2, with unequal weights, the spectral measure $P^{-1}\lambda$ of $P^{-1}\mathbf{X}$ gives unequal mass to e_1, e_2, so that $\mathcal{S}(P^{-1}\mu) = \mathcal{C}_1$ as for Example 4.2. Since $\mathcal{S}(\mu) = P\mathcal{S}(P^{-1}\mu)P^{-1}$, it follows that $\mathcal{S}(\mu) = \mathcal{C}_1$ as well. The construction in Example 4.5 yields $\mathcal{S}_0(\lambda) = \mathcal{D}_2$. Then $\mathcal{S}(\mu) = \mathcal{C}_2$ since the exponent $B = B_3$ is nilpotent, by Theorem 5.2 (b). In Example

4.6 we also have $\mathcal{S}_0(\lambda) = \mathcal{D}_2$, and then $\mathcal{S}(\mu) = \mathcal{C}_2$ by Theorem 5.2 (c). Example 4.7 has $\mathcal{S}(\mu) = \mathcal{D}_1$ since the spectral measure is symmetric with respect to reflection across the e_1-axis: $B = B_1$, and $F_0\lambda = \lambda$, but $-I\lambda \neq \lambda$. For Example 4.8 we begin with a change of coordinates $P^{-1}\mathbf{X}$ for the mean-centered process $\mathbf{X}$, where $P = F_0R_\theta$ with $\theta = -\pi/4$, so that $Pe_i = v_i$. The spectral measure $P^{-1}\lambda$ assigns equal weights of 0.4 to e_1 and e_2, and weight 0.2 to $(e_1 - e_2)/\sqrt{2}$. Now $\mathcal{S}_0(P^{-1}\lambda) = \mathcal{C}_1$. Since the exponent $D = P^{-1}BP$ is of the form B_1 in (5.8), Theorem 5.2 applies to show that $\mathcal{S}(P\mu) = \mathcal{C}_1$, and so $\mathcal{S}(\mu) = \mathcal{C}_1$ as well. Finally, in Example 4.9 a change of coordinates $Pv_i = e_i$ leads to $P^{-1}\mathbf{X}$ operator stable with exponent $B_1 = P^{-1}BP$ in Jordan form. Since the spectral measure λ gives equal weights of $1/4$ to the points $\pm c_i e_i$, we see that $P^{-1}\lambda(\pm c_i w_i) = 1/4$ where $Pe_i = w_i$. We can compute $w_1 = e_1$ and $w_2 = e_2 - (9/2)e_1$. Clearly the only symmetries of $P^{-1}\lambda$ are I and $R_\pi = -I$, so that $\mathcal{S}_0(P^{-1}\lambda) = \mathcal{C}_2$, and then Theorem 5.2 yields $\mathcal{S}(P^{-1}\mu) = \mathcal{C}_2$. Finally $\mathcal{S}(\mu) = P\mathcal{C}_2P^{-1} = \mathcal{C}_2$ since $\pm I$ commute with P. The shot noise representation in Theorem 3.1 shows that the symmetries in the distribution of $X(t)$ are also reflected in the sample paths. Hence, for example, the sample path in Figure 2 can be reflected through either axis, or both, to produce an equally likely path.

6. Operator self-similar processes

An operator stable Lévy process has stationary, independent increments. Some applications require dependent increments, nonstationarity, or both. In this section, we discuss more general operator self-similar processes, whose increments need not be independent or stationary. As usual, we assume that the operator self-similar process $\mathbf{X}$ is proper, and stochastically continuous, with $X(0) = 0$. Under these assumptions, the real parts of eigenvalues of the exponent B are positive [14, Theorem 4]. Let $\mathcal{S}(\mathbf{X})$ denote the symmetries of $\mathbf{X}$, i.e., the set of linear operators A in $\mathrm{GL}(\mathbb{R}^d)$ such that

$$\{AX(t)\}_{t\geq 0} \stackrel{fd}{=} \{X(t)\}_{t\geq 0}. \tag{6.1}$$

The symmetries form a compact subgroup of $\mathrm{GL}(\mathbb{R}^d)$ as long as $\mathbf{X}$ is proper. Symmetry is an important modeling consideration, and a useful guide to model selection. In particular, the natural symmetries of the system reflect the choice of exponent. Hudson and Mason [14, Theorem 2] proved that the possible exponents are given by

$$\mathcal{E}(\mathbf{X}) = B + T\mathcal{S}(\mathbf{X}), \tag{6.2}$$

where $B \in \mathcal{E}(\mathbf{X})$ is arbitrary and $T\mathcal{S}(\mathbf{X})$ is the tangent space of $\mathcal{S}(\mathbf{X})$ at the identity. Maejima [25] showed that one can always find a commuting exponent $B_c \in \mathcal{E}(\mathbf{X})$ such that $AB_c = B_cA$ for all $A \in \mathcal{S}(\mathbf{X})$. For any operator self-similar process, a change of coordinates puts the commuting exponent into Jordan form. The next result extends Theorem 5.1 to the more general case of operator self-similar processes. It shows that all symmetries are orthogonal in this coordinate system, and describes the possible symmetries depending on the Jordan form of the exponent.

Corollary 6.1. *Let $\mathbf{X} = \{X(t)\}_{t\geq 0}$ be a proper operator self-similar process in $\mathbb{R}^2$ with an exponent B given in the Jordan form* (5.8)*. Then the statements (i)–(iii) of Theorem 5.1 hold verbatim after replacing $\mathcal{S}(\mu)$ by $\mathcal{S}(\mathbf{X})$ and including $\mathcal{O}_2^+$ as a possible symmetry group in (ii)*

Proof. The exponents of a proper operator self-similar process are related to the symmetry group by (6.2), there always exists a commuting exponent, and the eigenvalues of any

exponent all have positive real part. These were the crucial facts used in the proof of Theorem 5.1. The rest of the proof is identical to Theorem 5.1, except that here we cannot exclude the case where $\mathcal{S}(\mu)$ is conjugate to $\mathcal{O}_2^+$, see Example 6.4 later in this section. □

Remark 6.2. As a simple extension of the construction in Remark 5.3, we can obtain an operator self-similar process in $\mathbb{R}^2$ with any exponent, and any admissible symmetry group. Take $X(t)$ as in Remark 5.3 and let $Y(t) = X(T(t))$ where $T(t)$ is a self-similar process (time change) with $T(at) = a^p T(t)$ (e.g., take $T(t) = t^p$). Then $Y(t)$ is operator self-similar with exponent $D = pB$. This, together with Example 6.4, also shows that $\mathcal{S}(\mathbf{X})$ can take every possible form listed in Corollary 6.1, which therefore provides a complete characterization in $\mathbb{R}^2$ of the possible symmetries of an o.s.s. process. An interesting and useful example of a self-similar process $\{T(t)\}$ with Hurst index $0 < \beta < 1$, which is not infinitely divisible or even Markovian, is given by the first passage or hitting time $T(t) = \inf\{u > 0 : D(u) > t\}$ of a stable subordinator $D(t)$ with $E(e^{-sD(t)}) = \exp(-cts^\beta)$. If we take $\{D(t)\}$ independent of the outer process $\mathbf{X}$, then the time changed process $Y(t) = X(T(t))$ has densities $h(x,t)$ that solve a space-time fractional multiscaling diffusion equation

$$\frac{\partial^\beta h(x,t)}{\partial t^\beta} = Lh(x,t)$$

where L is the generator of the operator stable semigroup, see for example [31, 32, 51]. This fractional diffusion equation has been applied to contaminant transport in heterogeneous porous media, where the process $Y(t)$ represents the path of a randomly selected contaminant particle. The order of the time fractional derivative β controls particle retention (sticking or trapping) while the exponent of the operator stable process codes the anomalous super-diffusion caused by long particle jumps. The inner process $T(t)$ is constant on intervals corresponding to jumps of the stable subordinator $D(t)$, the length of which is determined by the stable index β. A different governing equation pertains when the time change is not be independent of the outer process [4, 36]. Methods for simulating these non-Markovian subordinated processes have recently been developed by Magdziarz and Weron [22] and Zhang et al. [52] based on a simple random walk approximation of $\mathbf{X}$. It would be interesting to apply the results of this paper to improve those methods.

The alert reader will note that a shift is included in the definition of symmetry (5.1) for operator stable Lévy processes, which is natural, since the process definition (2.1) also includes a shift. For operator self-similar processes, the definition (1.1) does not include a shift, so it is natural that the symmetry definition (6.1) does not allow a shift. The following lemma relates these two definitions in the operator stable case.

Lemma 6.3. *Let $\mathbf{X} = \{X(t)\}_{t\geq 0}$ be a strictly operator stable Lévy process with exponent B. Suppose that 1 is not an eigenvalue of B. Then $\mathcal{S}(\mathbf{X}) = \mathcal{S}(\mu)$, where $\mu = \mathcal{L}(X(1))$.*

Proof. Since $\{X(t)\} \stackrel{fd}{=} \{AX(t)\}$ if and only if $X(1) \stackrel{d}{=} AX(1)$, we have $\mathcal{S}(\mathbf{X}) = \mathcal{S}_0(\mu)$, so it suffices to show that $\mathcal{S}(\mu) = \mathcal{S}_0(\mu)$ (see definitions (5.1) and (5.6)). Let $A \in \mathcal{S}(\mu)$, so that $AX(1)$ and $X(1) - b$ are identically distributed for some $b \in \mathbb{R}^d$. Since the real parts of eigenvalues of all exponents of μ are the same (see [30, Corollary 7.2.12]), we may take

B as a commuting exponent. Then, for every $t > 0$ we have

$$AX(t) \stackrel{d}{=} X(t) - tb \stackrel{d}{=} t^B X(1) - tb = t^B(AX(1) + b) - tb$$
$$= At^B X(1) + t^B b - tb \stackrel{d}{=} AX(t) + t^B b - tb.$$

Thus $(t^B - t)b = 0$ for all $t > 0$, and since 1 is not an eigenvalue of B, $b = 0$. Hence $A \in \mathcal{S}_0(\mu)$. The converse inclusion, $\mathcal{S}(\mu) \supset \mathcal{S}_0(\mu)$, is obvious. □

Full dimensional operator stable Lévy processes, and proper operator self-similar processes, form two distinct classes. Neither class is contained in the other: a drift can be added to an operator stable process, to break the operator self-similarity; a time change can make increments dependent or nonstationary, while maintaining operator scaling. Take $Z(t)$ a spherically symmetric Lévy process on $\mathbb{R}^d$ whose marginals are Cauchy. Then $b + Z(t)$ is an operator stable Lévy process, but it is not operator self-similar. The process $X(t) = Z(t^p)$ for $p > 1$ is operator self-similar but not Lévy. Remark 6.2 provides examples of operator self-similar processes for which none of the one-dimensional distributions are operator stable. The process $X(t) = vt + Z(t)$ is a strictly operator stable Lévy process and also a proper operator self-similar process. If we take $\mu = \mathcal{L}(X(1))$ then $\mathcal{S}(\mu) = \mathcal{O}_d$ but $\mathcal{S}_0(\mu) = \mathcal{S}(\mathbf{X})$ consists of the orthogonal transformations that fix the vector v. Remark 6.2 showed how to construct an operator self-similar process with any admissible symmetry group. The group $\mathcal{O}_2^+$ was included, even though it is not maximal, and hence cannot be the symmetry group of any probability measure (see Section 2). The next example shows that it is possible to have $\mathcal{S}(\mathbf{X}) = \mathcal{O}_2^+$ for some operator self-similar (not Lévy) processes. This illustrates the basic difference between the symmetries of a random vector, and those of a stochastic process. Process symmetries must also preserve finite dimensional distributions, and this further restriction affects the possible symmetry groups.

Example 6.4. Consider a complex valued process

$$X(t) = t^\beta \exp\left(i(\Theta + \log t)\right), \quad t > 0,$$

where $\beta > 0$, Θ is a uniform random variable on $[0, 2\pi]$ and $X(0) = 0$. Since for any $\phi \in \mathbb{R}$

$$\{e^{i\phi} X(t)\}_{t\geq 0} \stackrel{fd}{=} \{X(t)\}_{t\geq 0},$$

$\mathbf{X}$ as a process in $\mathbb{R}^2$,

$$X(t) = t^\beta \begin{bmatrix} \cos(\Theta + \log t) \\ \sin(\Theta + \log t) \end{bmatrix}$$

is a self-similar with index β and $\mathcal{O}_2^+ \subset \mathcal{S}(\mathbf{X})$. By (6.2), I and B_2 are exponents of $\mathbf{X}$ (B_2 with $b = \beta$ and arbitrary c). If $A \in \mathcal{S}(\mathbf{X})$ then

$$AX(1) \stackrel{d}{=} X(1)$$

which implies $A \in \mathcal{O}_2$. Thus $\mathcal{O}_2^+ \subset \mathcal{S}(\mathbf{X}) \subset \mathcal{O}_2$. Consider the process $\{F_0 X(t)\}_{t\geq 0}$, where F_0 is the reflexion with respect to the x-axis,

$$F_0 X(t) = t^\beta \begin{bmatrix} \cos(\Theta + \log t) \\ -\sin(\Theta + \log t) \end{bmatrix}.$$

If $F_0 \in \mathcal{S}(\mathbf{X})$, then for $t_1 = 1$ and $t_2 = e^{\pi/2}$ we would have

$$(F_0 X(1), F_0 X(e^{\pi/2})) \stackrel{d}{=} (X(1), X(e^{\pi/2})),$$

or

$$\left(\begin{bmatrix} \cos\Theta \\ -\sin\Theta \end{bmatrix}, e^{\beta\pi/2} \begin{bmatrix} -\sin\Theta \\ -\cos\Theta \end{bmatrix} \right) \stackrel{d}{=} \left(\begin{bmatrix} \cos\Theta \\ \sin\Theta \end{bmatrix}, e^{\beta\pi/2} \begin{bmatrix} -\sin\Theta \\ \cos\Theta \end{bmatrix} \right).$$

This equality written in $\mathbb{R}^4$ means

$$(\cos\Theta, -\sin\Theta, -\sin\Theta, -\cos\Theta) \stackrel{d}{=} (\cos\Theta, \sin\Theta, -\sin\Theta, \cos\Theta),$$

which is impossible since the sum of the first and the fourth random variables on the left hand side is 0, while on the right hand side is $2\cos\Theta$. Hence $F_0 \notin \mathcal{S}(\mathbf{X})$, which yields $\mathcal{S}(\mathbf{X}) = \mathcal{O}_2^+$.

Remark 6.5. Example 6.4 is consistent with the result that symmetry groups of probability measures must be maximal [28, Theorem 2], even though $\mathcal{O}_2^+$ is not a maximal subgroup of $\mathrm{GL}(\mathbb{R}^2)$. This is because, for A in $\mathcal{S}(\mathbf{X})$, we not only require $AX(t)$ identically distributed with $X(t)$ for a single $t > 0$, but also that $(AX(t_1), \ldots, AX(t_p))$ is identically distributed with $(X(t_1), \ldots, X(t_p))$ for all finite-dimensional distributions. We say that $\mathcal{O}_2^+$ acts diagonally in this case, and we identify A with corresponding element of $\mathrm{GL}(\mathbb{R}^{2p})$ defined by $(x_1, \ldots, x_p) \mapsto (Ax_1, \ldots, Ax_p)$ for $x_1, \ldots, x_p \in \mathbb{R}^2$. In Example 6.4 the diagonal action of $\mathcal{O}_2^+$ is a maximal subgroup of $\mathrm{GL}(\mathbb{R}^4)$, see the proof of Theorem 1 in [28].

Remark 6.6. In Examples 4.1, 4.3, 4.5 and 4.6 the operator stable process is centered, so that $\mathcal{S}(\mathbf{X}) = \mathcal{S}_0(\mu) = \mathcal{S}(\mu)$. In Example 4.7, we also have $\mathcal{S}(\mathbf{X}) = \mathcal{S}_0(\mu) = \mathcal{S}(\mu)$, since the drift vt is a fixed point of F_0. If we let $Y(t) = vt + X(t)$ for some $v \neq 0$, with $X(t)$ from Example 4.1, and write $\mu = \mathcal{L}(Y(1))$, then $\mathcal{S}(\mathbf{Y}) = \mathcal{S}_0(\mu) = \mathcal{C}_1$ is trivial, and strictly contained in $\mathcal{S}(\mu) = \mathcal{D}_2$. In Example 6.4 the symmetry group of the process $\mathcal{S}(\mathbf{X}) = \mathcal{O}_2^+$ is strictly contained in the symmetry group $\mathcal{S}(\mu) = \mathcal{O}_2$ of $\mu = \mathcal{L}(X(1))$.

References

[1] P. Abry, P. Gonçalves and J. Lévy Véhel, Scaling, fractals and wavelets, ISTE, London, 2009.

[2] S. Asmussen and J. Rosiński, Approximations of small jumps of Lévy processes with a view towards simulation. J. Appl. Probab. 38(2) (2001) 482–493.

[3] W. Barker and R. Howe, Continuous Symmetry: From Euclid to Klein. Amer. Math. Soc., 2007.

[4] P. Becker-Kern, M.M. Meerschaert and H.P. Scheffler, Limit theorems for coupled continuous time random walks. Ann. Probab. 32(1B) (2004) 730–756.

[5] P. Billingsley, Convergence of types in k-space. Z. Wahrsch. Verw. Geb. 5 (1966) 175–179.

[6] R. M. Blumenthal and R. K. Getoor, The dimension of the set of zeros and the graph of a symmetric stable process. Illinois J. Math. 6 (1962) 308–316.

[7] S. Cohen, C. Lacaux, and M. Ledoux, A general framework for simulation of fractional fields. Stoch. Proc. Appl. **118**(9) (2008) 1489–1517.

[8] S. Cohen and Rosiński. Gaussian approximation of multivariate Lévy processes with applications to simulation of tempered stable processes. Bernoulli, 13(1) (2007) 195–210.

[9] R. Cont and P. Tankov. Financial modelling with jump processes. Chapman & Hall/CRC, Boca Raton, Florida, 2004.

[10] P. Embrechts and M. Maejima, Self-similar Processes. Princeton University Press, 2002.

[11] D. Freedman, The Poisson approximation for dependent events. Ann. Prob. 2 (1974) 256–269.

[12] F A. Graybill. Matrices with applications in statistics. 2nd ed., Wadsworth, Belmont, Calif., 1983.

[13] D. Jansen and C. de Vries, On the frequency of large stock market returns: Putting booms and busts into perspective. Rev. Econ. Statist. 23 (1991) 18–24.

[14] W. N. Hudson and J. D. Mason. Operator-self-similar processes in a finite-dimensional space. Trans. Amer. Math. Soc. 273(1) (1982) 281–297.
[15] H.E. Hurst, R.P. Black, and Y.M. Simaika, Long-term Storage: An Experimental Study, Constable, London, 1965.
[16] A. Janicki and A. Weron, Simulation and Chaotic Behavior of α-Stable Stochastic Processes. Marcel Dekker, New York, 1994.
[17] Z. J. Jurek and J. D. Mason. Operator-Limit Distributions in Probability Theory. Wiley, New York, 1993.
[18] O. Kallenberg, Foundations of Modern Probability, 2nd ed., Springer-Verlag, New York, 2002.
[19] P. E. Kloeden and E. Platen. Numerical solution of stochastic differential equations. Springer-Verlag, New York, 1992.
[20] C. Lacaux, Series representation and simulation of multifractional Lévy motions. Adv. Appl. Probab., 36(1) (2004) 171–197.
[21] M. Loretan and P. Phillips, Testing the covariance stationarity of heavy tailed time series. J. Empirical Finance 1 (1994) 211–248.
[22] M. Magdziarz and A. Weron, Competition between subdiffusion and Lévy flights: A Monte Carlo approach, Phys. Rev. E 75 (2007) 056702.
[23] M. Maejima and J. D. Mason, Operator-self-similar stable processes. Stoch. Proc. Appl. 54 (1994) 139–163.
[24] M. Maejima. Operator-stable processes and operator fractional stable motions. Probab. Math. Statist., 15 (1995) 449–460.
[25] M. Maejima. Norming operators for operator-self-similar processes. Trends Math., 287–295, Birkhuser, Boston, 1998.
[26] B. B. Mandelbrot, The fractal geometry of nature, W. H. Freeman, San Francisco, Calif., 1982.
[27] M.M. Meerschaert and H.P. Scheffler, One dimensional marginals of operator stable laws and their domains of attraction, Publ. Math. Debrecen 55(3–4) (1999) 487–499.
[28] M. M. Meerschaert and J. A. Veeh. Symmetry groups in d-space. Statist. Probab. Lett. 22 (1995) 1–6.
[29] M. M. Meerschaert and H.-P. Scheffler, Sample cross-correlations for moving averages with regularly varying tails. J. Time Series Anal. 22(4) (2001) 481–492.
[30] M. M. Meerschaert and H.-P. Scheffler, Limit Distributions for Sums of Independent Random Vectors: Heavy Tails in Theory and Practice. Wiley, New York, 2001.
[31] M. M. Meerschaert,D. A. Benson and B. Baeumer, Operator Lévy motion and multiscaling anomalous diffusion. Phys. Rev. E 63 (2001) 1112–1117.
[32] M.M. Meerschaert, D.A. Benson, H.P. Scheffler and B. Baeumer, Stochastic solution of space-time fractional diffusion equations. Phys. Rev. E 65 (2002) 1103–1106.
[33] M.M. Meerschaert and H.P. Scheffler, Portfolio modeling with heavy tailed random vectors. Handbook of Heavy-Tailed Distributions in Finance, 595–640, S. T. Rachev, Ed., Elsevier, New York, 2003.
[34] M. M. Meerschaert and Y. Xiao, Dimension results for sample paths of operator stable Levy processes. Stoch. Proc. Appl. 115(1) (2005) 55–75.
[35] M.M. Meerschaert and E. Scalas, Coupled continuous time random walks in finance. Physica A: Statistical Mechanics and Its Applications 370 (2006) 114–118.
[36] M.M. Meerschaert and H.-P. Scheffler, Triangular array limits for continuous time random walks. Stoch. Proc. Appl. 118 (2008) 1606–1633.
[37] F. J. Molz, H. Rajaram and S. Lu, Stochastic fractal-based models of heterogeneity in subsurface hydrology: Origins, applications, limitations, and future research questions. Rev. Geophys. 42 (2004) RG1002.
[38] M. Park and J.H. Cushman, On upscaling operator-stable Lévy motions in fractal porous media. J. Comput. Phys., 217(1) (2006) 159–165.
[39] M. Park and J.H. Cushman, Operator-stable Lévy motions and renormalizing the chaotic dynamics of microbes in anisotropic porous media. J. Statist. Mechanics 2009(2) (2009) P02039.
[40] W.E. Pruitt and S.J. Taylor, Sample path properties of processes with stable components. Z. Wahrsch. verw. Geb. 12 (1969) 267–289.
[41] S. Rachev and S. Mittnik, Stable Paretian Models in Finance, Wiley, Chichester, 2000.
[42] B.S. Rajput and J. Rosiński. Spectral representations of infinitely divisible processes. Probab. Th. Rel. Fields 82 (1989) 451–487.

[43] D.M. Reeves, D.A. Benson, M.M. Meerschaert, H.P. Scheffler, Transport of conservative solutes in simulated fracture networks 2. Ensemble solute transport and the correspondence to operator-stable limit distributions, Water Resour. Res. 44 (2008) W05410.
[44] J. Rosiński, On series representations of infinitely divisible random vectors. Ann. Probab. 82 (1990) 405–430.
[45] J. Rosiński. Series representations of Lévy processes from the perspective of point processes. Lévy processes, 401–415. Birkhäuser, Boston, 2001.
[46] J. Rosiński, Tempering stable processes, Bernoulli 13 (2007) 195–210.
[47] K.-I. Sato, Strictly operator-stable distributions. J. Multivariate Anal. 22 (1987) 278–285.
[48] K.-I. Sato, Lévy Processes and Infinitely Divisible Distributions, Cambridge University Press, 1999.
[49] E. Scalas, R. Gorenflo, F. Mainardi, and M.M. Meerschaert, Speculative option valuation and the fractional diffusion equation, Fractional Derivatives and Their Applications, 265–274, A. Le Mehauté, J. A. Tenreiro Machado, J. C. Trigeassou and J. Sabatier, Eds., Ubooks, Germany, 2005.
[50] O. Sheluhin, S. Smolskiy and A. Osin, Self-Similar Processes in Telecommunications, Wiley, New York, 2007.
[51] Y. Zhang, D.A. Benson, M.M. Meerschaert, E. M. LaBolle, and H.P. Scheffler. Random walk approximation of fractional-order multiscaling anomalous diffusion. Phys. Rev. E 74(2) (2006) 6706–6715.
[52] Y. Zhang, M.M. Meerschaert, B. Baeumer, Particle tracking for time-fractional diffusion, Phys. Rev. E 78(3) (2008) 036705.

Serge Cohen, Université de Toulouse, Université Paul Sabatier, Institut de Mathématiques de Toulouse. F-31062 Toulouse. France.
E-mail address: Serge.Cohen@math.univ-toulouse.fr
URL: http://www.math.univ-toulouse.fr/∼cohen/

Mark M. Meerschaert, Department of Statistics and Probability, Michigan State University, East Lansing, MI 48824
E-mail address: mcubed@stt.msu.edu
URL: http://www.stt.msu.edu/∼mcubed

Jan Rosiński, Department of Mathematics, University of Tennessee, Knoxville, TN 37996, USA.
E-mail address: rosinski@math.utk.edu
URL: http://www.math.utk.edu/∼rosinski/